

# < EQUALITY >

Efficient QUantum ALgorithms for IndusTrY

WP4 Proof-of-concept / Energy Storage

## D4.1 Problem Specification Sheets (Energy Storage)

Version: 1.00

Date: 28/04/2023

**AIRBUS**

Capgemini

 DA VINCI LABS

 **Fraunhofer**  
ENAS

 **DLR**  
Deutsches Zentrum  
für Luft- und Raumfahrt  
German Aerospace Center

*Inria*

 **Universiteit  
Leiden**  
The Netherlands

 **PASQAL**

## Document control

<b>Project title</b>	Efficient QUantum ALgorithms for IndusTrY
<b>Project acronym</b>	EQUALITY
<b>Call identifier</b>	HORIZON-CL4-2021-DIGITAL-EMERGING-02
<b>Grant agreement</b>	101080142
<b>Starting date</b>	01/11/2022
<b>Duration</b>	36 months
<b>Project URL</b>	<a href="http://equality-quantum.eu">http://equality-quantum.eu</a>
<b>Work Package</b>	WP4 Proof-of-concept trials / energy storage
<b>Deliverable</b>	D4.1 problem specification sheet (energy storage)
<b>Contractual Delivery Date</b>	M6
<b>Actual Delivery Date</b>	M6
<b>Nature<sup>1</sup></b>	R
<b>Dissemination level<sup>2</sup></b>	PU
<b>Lead Beneficiary</b>	DLR
<b>Editor(s)</b>	Max Schammer (DLR), Xiao HU (ENAS), Andreas Zienert (ENAS), Franziska Wolff (CAP)
<b>Contributor(s)</b>	Lorenzo Cardarelli (QC), Panagiotis Barkoutsos (QC)
<b>Reviewer(s)</b>	Birger Horstmann (DLR), Wael Yahyaoui (CAP)
<b>Document description</b>	This deliverable defines specific problem statements for each of the four trials (Predictive models for battery design and fuel cells; Simulations of solid oxide fuel cells; Materials discovery for battery design; Atomistic models for fuel cell simulation) including detailed descriptions of the problem scenario, the chosen methods, its implications, and its impact on the different stakeholders.

<sup>1</sup>R: Document, report (excluding the periodic and final reports); DEM: Demonstrator, pilot, prototype, plan designs; DEC: Websites, patents filing, press & media actions, videos, etc.; DATA: Data sets, microdata, etc.; DMP: Data management plan; ETHICS: Deliverables related to ethics issues.; SECURITY: Deliverables related to security issues; OTHER: Software, technical diagram, algorithms, models, etc.

<sup>2</sup>PU – Public, fully open, e.g. web (Deliverables flagged as public will be automatically published in CORDIS project's page); SEN – Sensitive, limited under the conditions of the Grant Agreement; Classified R-UE/EU-R – EU RESTRICTED under the Commission Decision No2015/444; Classified C-UE/EU-C – EU CONFIDENTIAL under the Commission Decision No2015/444; Classified S-UE/EU-S – EU SECRET under the Commission Decision No2015/444

## Version control

Version	Editor(s) Contributor(s) Reviewer(s)	Date	Description
0.4	Max Schammer (DLR)	14/03/2023	Intermediate document finished.
0.5	Birger Horstmann (DLR)	11/04/2023	Intermediate document approved by the reviewer.
0.8	Max Schammer (DLR) Xiao HU (ENAS) Andreas Zienert (ENAS) Franziska Wolff (CAP)	20/04/2023	Document finished by editor.
0.98	Birger Horstmann (DLR)	27/04/2023	Document approved by reviewer.
1.0	Wael Yahyaoui	28/04/2023	Document released by Project Coordinator.

## Abstract

A quantum revolution is unfolding, and European scientists are on the lead. Now, it is time to take decisive action and transform our scientific potential into a competitive advantage. Achieving this goal will be critical to ensuring Europe’s technological sovereignty in the coming decades.

EQUALITY brings together scientists, innovators, and prominent industrial players with the mission of developing cutting-edge quantum algorithms to solve strategic industrial problems. The consortium will develop a set of algorithmic primitives which could be used as modules for various industry-specific workflows. These primitives include differential equation solvers, material simulation algorithms, quantum optimisers, etc.

To focus our efforts, we target eight paradigmatic industrial problems. These problems are likely to yield to early quantum advantage and pertain to the aerospace and energy storage industries. They include airfoil aerodynamics, battery and fuel cell design, space mission optimisation, etc. Our goal is to develop quantum algorithms for real industrial problems using real quantum hardware. This requires grappling with the limitations of present-day quantum hardware. Thus, we will devote a large portion of our efforts to developing strategies for optimal hardware exploitation. These low-level implementations will account for the effects of noise and topology and will optimise algorithms to run on limited hardware.

EQUALITY will build synergies with Quantum Flagship projects and Europe’s thriving ecosystem of quantum start-ups. Use cases will be tested on quantum hardware from three of Europe’s leading vendors and two high performance computing (HPC) centres. The applications targeted have the potential of creating billions of euros for end-users and technology providers over the coming decades. With EQUALITY, we aim at playing a role in unlocking this value and placing Europe at the centre of this development. The project gathers 9 partners and has a budget of €6M over 3 years.

## Consortium

The EQUALITY consortium members are listed below.

Legal Name on Grant Agreement	Short name	Country
CAPGEMINI DEUTSCHLAND GMBH	CAP	DE
QU & CO AI BV	QC	FR
AIRBUS OPERATIONS GMBH	AOG	DE
DEUTSCHES ZENTRUM FUR LUFT - UND RAUMFAHRT EV (DLR)	DLR	DE
FRAUNHOFER GESELLSCHAFT ZUR FORDERUNG DER ANGEWANDTEN FORSCHUNG EV (FHG)	ENAS	DE
INSTITUT NATIONAL DE RECHERCHE EN INFORMATIQUE ET AUTOMATIQUE (INRIA)	INRIA	FR
UNIVERSITEIT LEIDEN (ULEI)	ULEI	NL
DA VINCI LABS	DVL	FR

## Disclaimer

This document does not represent the opinion of the European Union or European Commission, and neither the European Union nor the granting authority can be held responsible for any use that might be made of its content.

This document may contain material, which is the copyright of certain EQUALITY consortium parties, and may not be reproduced or copied without permission. All EQUALITY consortium parties have agreed to full publication of this document. The commercial use of any information contained in this document may require a license from the proprietor of that information.

Neither the EQUALITY consortium, nor a certain party of the EQUALITY consortium warrant that the information contained in this document is capable of use, nor that use of the information is free from risk and does not accept any liability for loss or damage suffered by any person using this information.

## Acknowledgement

This document is a deliverable of EQUALITY project. This project has received funding from the European Union's Horizon Europe research and innovation programme under grant agreement N° 101080142.

## Abbreviations

WP	Work package
1D + 1D	1 dimensional + 1 dimensional
2D	Two dimensional
APU	Auxiliary power unit
B3LYP	Becke, 3-parameter, Lee-Yang-Parr
CAE	Computer aided engineering
CCSD(T)	Coupled cluster with full treatment singles and doubles and approximate treatment of connected triples
CFD	Computational Fluid Dynamic
DFT	Density functional theory
DQC	Differentiable quantum circuit
EC	Ethylene carbonate
EDL	Electrochemical double layer
FC	Fuel cell
(q)GANs	(quantum) Generative Adversarial Networks
GGA	Generalized gradient approximation
hBN	Hexagonal boron nitride
HF	Hartree-Fock
HK	Hohenberg-Kohn
HPC	High performance computing
KS	Kohn and Sham
LIB	Lithium-ion battery
LiPS	Lithium polysulfide species
Li-S	Lithium-sulphur
LiTFSI	Lithium salt bis(trifluoromethane)-sulfonimide
LSDA	Local spin density approximation
MD	Molecular dynamics
NEB	Nudged elastic band
NISQ	Noisy intermediate quantum computer
NMC	Nickel manganese cobalt
NVT	Canonical ensemble (constant amount of substance N, volume V, and temperature T)
ORR	Oxygen reduction reaction
PBE	Perdew-Burke-Ernzerhof

PEMFC	Proton-exchange membrane fuel cell
QNN	Quantum neural network
QQM	Quantum quantile mechanics
RT	Rational thermodynamics
SDE	Stochastic differential equations
SEI	Solid-electrolyte interphase
SOFC	Solid oxide fuel cell
TMD	Transition metal dichalcogenides
UAV	Unmanned aerial vehicles
vdW	Van der Waals
VQA	Variational quantum algorithm
YSZ	Yttria-stabilized zirconia

## Table of Contents

<b>DOCUMENT CONTROL</b> .....	<b>2</b>
<b>VERSION CONTROL</b> .....	<b>3</b>
<b>ABSTRACT</b> .....	<b>4</b>
<b>CONSORTIUM</b> .....	<b>4</b>
<b>DISCLAIMER</b> .....	<b>5</b>
<b>ACKNOWLEDGEMENT</b> .....	<b>5</b>
<b>ABBREVIATIONS</b> .....	<b>6</b>
<b>LIST OF FIGURES</b> .....	<b>9</b>
<b>1. EXECUTIVE SUMMARY</b> .....	<b>10</b>
<b>2. QUANTUM IN ENERGY STORAGE SYSTEMS</b> .....	<b>11</b>
<b>3. APPLIED METHODOLOGY</b> .....	<b>12</b>
<b>4. ELECTROCHEMICAL BENCHMARK SYSTEMS</b> .....	<b>16</b>
4.1. THE LITHIUM SULPHUR BATTERY .....	16
4.2. FUEL CELLS AND THE SOLID OXIDE FUEL CELL.....	18
<b>5. PARTIAL DIFFERENTIAL EQUATION SOLVERS FOR BATTERY AND FUEL CELL DESIGN (FIRST USE CASE) ..</b>	<b>21</b>
5.1. CONTINUUM SIMULATIONS OF LITHIUM SULPHUR BATTERIES .....	21
5.2. CONTINUUM FUEL CELLS SIMULATIONS.....	31
<b>6. SOLID OXIDE FUEL CELL OPTIMIZATION AND BATTERY MATERIAL DISCOVERY (SECOND AND SIXTH USE CASE) .....</b>	<b>37</b>
6.1. MATERIALS DISCOVERY FOR BATTERY DESIGN .....	37
6.2. ATOMISTIC MODELS FOR FUEL CELL SIMULATION .....	47
<b>7. BIBLIOGRAPHY</b> .....	<b>51</b>



## List of figures

FIGURE 1 ILLUSTRATION OF THE MULTI-SCALE APPROACH FOR THE EXAMPLE OF A BATTERY. ....	13
FIGURE 2 COMPARISON OF SPECIFIC ENERGY DENSITY OF DIFFERENT BATTERY TYPES. A) COMPARISON OF GRAVIMETRIC ENERGY DENSITY OF LIBS AND LI-S BATTERIES (DATA TAKEN FROM [20]). B) COMPARISON OF VOLUMETRIC AND GRAVIMETRIC ENERGY DENSITY OF LI-S AND LIB (DATA TAKEN FROM [21]). ....	16
FIGURE 3 ILLUSTRATION OF THE SET-UP AND TYPICAL VOLTAGE PROFILE OF A LI-S BATTERY. A) DURING DISCHARGE, LI-IONS MOVE TOWARDS THE SULPHUR CATHODE, WHERE LITHIUM POLYSULFIDES FORM AND MOVE BETWEEN THE ELECTRODES VIA A SHUTTLE MECHANISM. B) VOLTAGE PROFILE FOR DISCHARGING / CHARGING OF A LI-S BATTERY (DATA WAS TAKEN FROM [1]). ....	18
FIGURE 4 MARKET OVERVIEW OF FCS WORLDWIDE (SOURCE [41]). ....	19
FIGURE 5 ILLUSTRATION OF THE SET-UP OF A SOFC.....	19
FIGURE 6 ILLUSTRATION OF THE CONTINUUM HYPOTHESIS. ....	23
FIGURE 7 MODULAR SET-UP FOR THE ELECTRONEUTRAL CELL SIMULATIONS. ....	28
FIGURE 8 ILLUSTRATION FOR THE MULTI-PHASE REACTIONS OCCURRING AT THE SOFC ANODE. ....	32
FIGURE 9 MODULAR APPROACH FOR THE MODELLING OF THE SOFC. ....	35

## 1. EXECUTIVE SUMMARY

This document is a deliverable of the EQUALITY project, funded under grant agreement number 101080142.

This deliverable, “D4.1 Problem Specification Sheets (Energy Storage),” is part of Work Package 4 (WP4) “Proof-of-concept trials / energy storage”. The focus of activities in WP4 lies on testing the algorithms developed in WP1 for specific use cases from energy storage. The objectives of this WP are to perform simulation trials for quantum algorithms from the WP1 based on well-defined problems. The trials follow a stepwise structure. First, simulations will be performed on ideal emulators, where the number of qubits is increased incrementally. Next, noise and topology factors will be included. Finally, emulators based on real quantum hardware will be applied. To assess the performance and map the boundary of classical capabilities, state-of-the-art classical computations will be conducted in parallel. The practical impact will be evaluated using the strategies developed in the WP2.

This deliverable presents specific use cases from energy storage, which constitute the test environment for the quantum algorithms developed in WP 1. It provides a concise overview over the technological and scientific state of electrochemical energy storage and presents an introduction into the different modelling methodologies of electrochemical systems and into the quantum approach. The deliverable identifies two promising benchmark system, which form the basis of the two use cases discussed in this document. Both systems are highly relevant from a scientific and industrial perspective and are very well suited for the planned activities of the EQUALITY project. The first use case defined in these deliverable focuses on the continuum modelling of the two electrochemical systems, and how quantum algorithms can be applied to solve the differential equations of the continuum description numerically. The second use case focuses on the combination of the atomistic modelling of the two electrochemical systems, with the quantum approach. Here, an emphasis is put on materials discovery. For both use cases, detailed strategies for the quantum activities are described. A modular approach based on well-defined intermediate steps ensures that the progress and performance of the quantum algorithms can be screened effectively. This also allows to adjust the quantum approach depending on progress, and in the case that technical problems are identified.

This deliverable D4.1 is followed by performance report D4.2 at M18, and performance report D4.3 at M36. Both of these two deliverables will focus on the evaluation of the activities outlined in this deliverable.

## 2. Quantum in energy storage systems

Mobile and stationary devices for energy storage play a fundamental role in our modern society. They can be found in various everyday devices, from mobile phones to electrified vehicles. Also, they are crucial for the transition towards a carbon-neutral economy. In this context, electrochemical systems like batteries or fuel cells, play a pivotal role, and there exists an increasing demand for better and more durable devices. This constitutes a significant research stimulus, which pertains to improving already existent technologies, but, also, to the development of novel systems.

These ambitious goals represent a heterodox problem landscape for a variety of research communities, ranging from industry and technology to fundamental science. This involves exploiting and combining expertise which is specific to the individual research communities involved in this endeavour. However, because the used methodologies are based on a variety of techniques and methodologies, this can be a challenging task. Consequently, it is crucial for achieving the goals to apply a holistic research approach. This strategy involves experimental techniques and methods, and modelling. Computer simulations based on theoretical models play a vital role for achieving these goals.

In almost all cases, such theoretical models consist of sets of coupled (nonlinear) partial differential equations. Because these are hard to solve analytically, they must be solved using numerical simulations instead. However, even for smaller systems with a reduced degree of complexity, such numerical simulations consume large amounts of computational resources. In many cases, these resources lie beyond the capabilities of classical computers.

Quantum computers constitute a promising approach for solving differential equations efficiently. In particular, because of their much higher computational power, they have the potential to overcome many classical restrictions.

The effort to bring quantum computers to the forefront of solving differential equations, relies on two related issues. First, it involves the development of novel algorithms which are customized to using them on quantum hardware. Because the quantum hardware operates on a conceptually different physical set-up, software tools developed for classical computers are not applicable. However, the pre-requisite for using quantum algorithms to solve differential equations is the availability of highly advanced quantum hardware. Therefore, the development of more stable quantum hardware is a precondition to harvest their extensive computational power in numerical simulations.

Currently, there exist hardware realizations for quantum computers of limited size. Even though they consist only of a few qubits, they are promising hardware solutions, nevertheless. Most importantly, they allow the successful implementation of novel quantum algorithms. This limited hardware infrastructure constitutes a testbed for developing and evaluating quantum software. In particular, quantum algorithms for solving linear [2] and non-linear systems of differential equations [3] have been reported recently. In addition, novel quantum algorithms for solving non-linear differential equations, which are tailor-cut to limited quantum hardware, have been developed [4,5].

Altogether, the advent of quantum computing implies many promising developments that are beneficial for the field of energy storage.

### 3. Applied methodology

In this section we present an overview over our holistic modelling approach, including the different modelling methodologies involved in the use cases, and discuss our strategy for the development of novel quantum algorithms. Furthermore, we motivate and define the two benchmark electrochemical systems studied in the two use cases. Finally, we outline the structure of this document.

#### *Modelling Methodology*

The modelling of batteries and fuels requires considering phenomena on multiple length scales, ranging from the microscopic scale (nm scale) up to the mesoscopic scale ( $\mu\text{m}$  scale) and up to the macroscopic scale (mm scale). Each length scale has its own physics framework and mathematical techniques. Phenomena on the nanoscale are usually described via chemical reactions between individual atoms or molecules. Here, atomistic models based on quantum mechanics are usually applied. In contrast, mesoscopic ( $\mu\text{m}$ -scale) and macroscopic (mm-scale) phenomena are usually described via theoretical methods based on continuum models. Consequently, the theoretical description of the complete system requires a holistic theoretical framework, which consistently couples the atomistic description with the continuum description. This can be achieved via the consistent parameterization of the continuum model based on theoretical results from the atomistic methods. Figure 1 illustrates this multi-scale approach for the example of a battery system. Here, the macroscopic system (mm-scale) is a battery, which, in a simplified description, consists of two electrodes and an electrolyte in between. For the description of transport processes, i.e., migration, convection, and diffusion, it suffices to focus on an arbitrary volume element within the bulk electrolyte on the mesoscopic scale ( $\mu\text{m}$ -scale). On this length scale, one can safely neglect the particle nature of the electrolyte and apply methods from non-equilibrium thermodynamics. However, there are important effects which happen on smaller length scales. For example, the interface between the electrode material (solid phase) and the electrolyte (here, liquid phase) where passivation layers (e.g., the solid-electrolyte interphase, SEI) and the electrochemical double layer (EDL) are formed, play a vital role for the performance of the battery. Typically, the EDL ranges over some nanometers, as illustrated in Figure 1. The same arguments apply to fuel cells as well.

The consistent modelling of the complete electrochemical system, however, results in a theoretical framework, which allows to draw insight into the functioning and the performance of the system. In particular, the theoretical framework takes the form of a fully coupled set of (algebraic) non-linear partial differential equations. These describe the evolution of the system based on experimentally validated parameters and boundary conditions.

To obtain quantitative results, the transport equations must be solved numerically. However, in most cases, these equations are too difficult to solve manually, although analytical techniques may allow to derive qualitative results. Thus, they must be solved numerically based on computer simulations. Because of complex couplings between effects happening on different length scales and over different time scales, the simulation of electrochemical systems can be numerically challenging. Indeed, even for small electrochemical systems composed of a few molecules, the numerical complexity can become problematic for classical computers. Hence, for many systems, such simulations require the computational power of computer-clusters or supercomputers (high-performance computing / HPC) and require a highly advanced software infrastructure to process the resulting data (parallel programming).

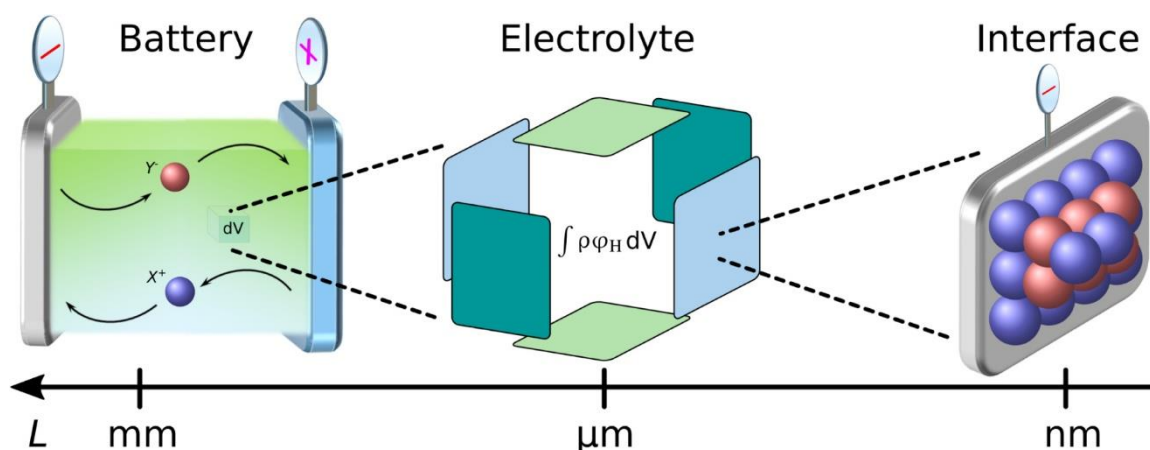


Figure 1 Illustration of the multi-Scale approach for the example of a battery.

Therefore, the theoretical description of electrochemical systems can benefit greatly from the development of novel simulation tools and novel computer hardware.

#### Quantum Methodology

Quantum computing constitutes a highly dynamical field of research which has many promising applications. In the context of this document, it has the potential to significantly push the applicability of computer-based numerical simulations of electrochemical systems. However, to transform this scientific potential into broadly available and commercialized end-products, two key factors must be addressed. The first factor is the realization of highly efficient quantum hardware. The second factor is the development of novel quantum algorithms, to harvest the computational power of the quantum hardware. In this project, different types of hardware will be considered (emulators, trapped ions, Rydberg atoms and superconducting qubits). However, the focus of this project lies on the development of quantum algorithms for real industrial problems, which run on real quantum hardware. For this purpose, a group of eight core algorithms has been identified, which constitutes a set of quantum algorithms with wide applicability, see Table 1.

Differential equation (DE) solvers	Stochastic DE solvers	Quantum generative models	Quantum chemistry simulations
Simulations for periodic materials	Quantum evolution kernel methods	Non-kernel quantum ML techniques	Gibbs state-based optimization

Table 1 Summary of core algorithms identified in this project.

However, present-day devices of quantum hardware have limitations due to limited numbers of qubits, and noise-sensitive circuits. From this arises the problem of how to implement quantum algorithms effectively on limited real hardware. Thus, the activities related to the development of the core quantum algorithms put emphasis on finding strategies of how to

ideally exploit scarce and noisy quantum resources. This effort is bundled in a set of six optimal hardware exploitation methods see Table 2.

Divide-and-conquer strategies	Optimal qubits routing algorithms	Exploitation of analogue mode simulations
Efficient trap-based noise characterisation	Logic-based methods for circuit optimisation	Machine learning-based methods for circuit optimization

*Table 2 Hardware exploitation methods.*

Solving differential equations (DE) is very important in virtually all engineering and science disciplines. As outlined above, there exists hope that quantum computers imply novel techniques for solving DEs efficiently. Recently, a novel variational quantum algorithm (VQA) for solving DEs on NISQ devices has been reported by consortium member QC [4]. This approach is based on a deep neural network, which is used to derive trial solutions of a given DE via the method of backpropagation [5]. Hardware requirements of the quantum neural network (QNN) employed for the expression of the trial solutions are reduced via a specific Differential Quantum Circuit (DQC) strategy. Solving stochastic differential equations (SDEs) is even more challenging due to the issue of dimensionality, although there has been made some progress in recent years [6]. An alternative strategy used in this project, called Quantum quantile mechanics (QQM), is based on quantile mechanics [7], by leveraging neural representations of quantile distribution functions [8]. The QQM approach is closely related to the machine learning tools of the (quantum) Generative Adversarial Networks (qGANs or GANS) for generative modelling. Gibbs-states originate from statistical mechanics and offer a description for systems in thermal equilibrium. They are closely related to optimization problems by the so-called mirror-descent process. Thus, Gibbs-state tasks can be transformed to optimization problems [9]. However, because optimization algorithms are heavily noise dependent, the development of noise-tolerant optimization algorithms is crucial for this task. Another very important topic is to develop quantum algorithms for quantum chemistry calculations on NISQ devices. Quantum chemistry relies on solving Schrödinger’s equation numerically. In most cases, this is done using the Born-Oppenheimer approximation for the electronic structure, where the nuclei and electronic degrees of freedom are decoupled. The “wave-function”-approach, which is based on the description of the electronic wave-function, leads to very accurate results but is computationally demanding. For this reason, the electronic structure is often calculated based on the much simpler electronic density function via the so-called Density Functional Theory (DFT). However, it is the hope that quantum computing can be employed for highly efficient wave-function calculations [10]. Present-day NISQ algorithms for quantum chemistry are based on the Coupled Cluster (CC) theory. Based on this approach, consortium member QC recently proposed the novel “Unitary Coupled Cluster with Double excitations” (pUCCD) quantum algorithm [11]. This quantum algorithm shows promising results for implementing quantum chemistry simulations on NISQ devices. Also, the development of novel quantum machine learning tools is highly relevant for many fields research, ranging from, e.g., chemistry or bioinformatics to social network analysis or computer vision.

However, beneath the development of quantum algorithms, hardware efficient implementations are crucial. Variational approaches have been developed to exploit scarce quantum resources by offsetting parts of a computation to classical devices. However, it is yet unknown how to distribute the workflow between classical and quantum processors. One solution to this problem was pioneered by Consortium member ULEI [12–14]. Their “divide

and conquer“ approach reduces, or “cuts”, classical algorithms into subroutines, which are small enough to be tackled by quantum processors. This basic principle has led to refined variations of the cutting approach. In addition, topological constraints constitute obstacles for the execution of quantum circuits on real quantum processors. Qubits which are topologically not connected can be linked to each other via a process called qubit routing. However, this process involves computational costs by itself, and hence a delicate balance must be identified. Furthermore, the inherent presence of noise in quantum devices often hinders a reliable and efficient performance of quantum computations on NISQ machines. To minimize the negative influence of the noise, the development of noise-characterizing and noise-predicting models is crucial. Recently, EQUALITY partner INRIA has proposed a novel efficient protocol relying on trap-based verification techniques to tackle this issue [15]. Noise resilience of quantum hardware can also be studied using machine learning algorithms based on classical simulations. However, there exist also type-specific problems of quantum hardware. Thus, to boost the performance of quantum algorithms on different quantum platforms, e.g. Ryberg atom platforms, the quantum algorithms must be customized.

### *Use Case Specifications*

The above discussion provides an overview of the general landscape of electrochemical systems which have been successfully commercialized in the context of energy storage and provides an overview over the atomistic and continuum modelling methodologies, as well as over the quantum approach. This discussion lays the ground for the definition of the specific use cases, which shall be investigated in the activities outlined in this document. We designate two specific electrochemical systems on which the research activities will focus, and which constitute the use cases. We cover the two main types of electrochemical systems in the context of energy storage and choose one battery system and one type of fuel cell for these two benchmark systems. From the battery landscape, we choose the lithium sulphur system, and from the fuel cell landscape, we choose the solid oxide fuel cell. Both systems are highly relevant from an applications-based point of view, as well as from a scientific perspective. The lithium sulphur battery is a very promising battery system and has been subject to intense research in the last decades. Solid oxide fuel cells have already been commercialized and offer many auspicious properties for improvement. In addition, both systems are ideally suited to be investigated via a holistic modelling approach discussed above.

These two electrochemical benchmark systems will both be studied from a continuum-modelling perspective, and from an atomistic perspective. This holistic approach constitutes the two use cases. The first use case focuses on the application of quantum algorithms to the continuum modelling of the two benchmark systems. The second use case focuses on the application of quantum algorithms to the atomistic modelling methodology.

### *Structure of the Document*

We structure this document into three main parts. First, in section 4, we present a detailed description of the two benchmark electrochemical systems which will be studied in the two use cases. In the next two sections, we define the two use cases. For both use cases, this discussion includes a detailed description of the problem scenario, the applied methods, as well as the expected implications and impact on the stakeholders. In section 5 we describe the first use case, which focuses on continuum modelling. Next, in section 6, we focus on the atomistic modelling methodology. However, to highlight the complementarity of these two modelling approaches, we divide each use case into two subcases. One subcase focuses on the lithium sulphur system and one subcase focuses on the solid oxide fuel cell.

## 4. Electrochemical Benchmark Systems

In this section, we describe the two electrochemical systems on which the use cases defined in this deliverable will be focused on. First, in section 4.1, we present a detailed description of the lithium sulphur battery. Second, in section 4.2, we present a detailed description of the solid oxide fuel cell. Both systems constitute ideal electrochemical systems to be discussed in the two use cases.

### 4.1. The Lithium Sulphur Battery

Lithium ion batteries (LIBs) were successfully commercialized in the 1990s, and have rapidly gained a dominant position in the worldwide energy market that lasts until today, due to the combination of high specific power and high specific energy [16]. LIBs are based on the use of Li-intercalation compounds as electrodes, where the Li ions migrate across the electrolyte located between the two electrode host structures. The advantageous properties of Li-electrochemistry result from basic atomic properties of the lithium via a low molecular weight and small ionic radius of lithium. Furthermore, it has a low redox potential, which enables high-output voltages leading to high energy densities. Also, LIBs exhibit long cycle life and rate capability. However, with the ever increasing demand for enhanced device duration, and in the context of a broadened application landscape for batteries, e.g. unmanned aerial vehicles or electrified cars, the LIB technology has reached its limitations [17,18]. Also, LIBs depend crucially on a variety of components which do not exist in abundance. Hence, the availability of these materials is subject to a highly dynamical economic and political landscape [19].

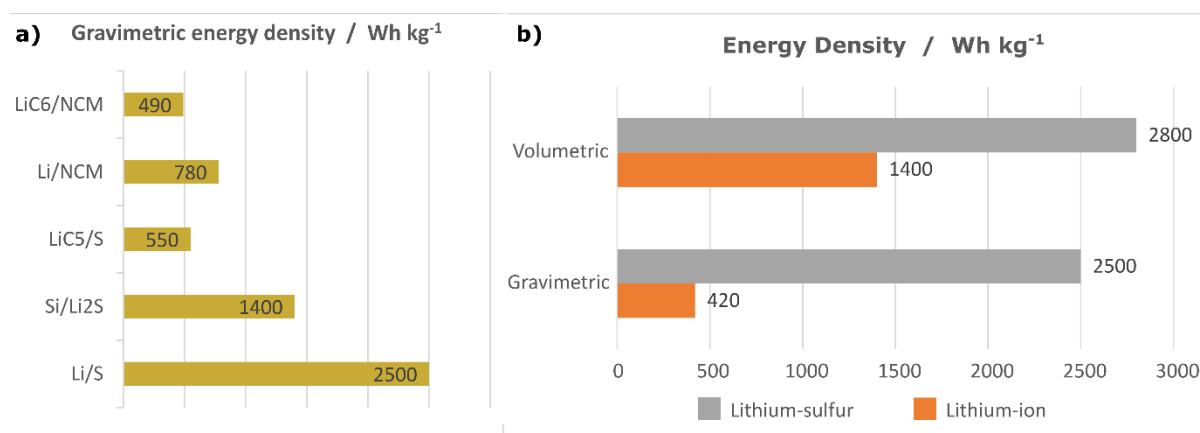


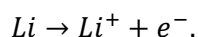
*Figure 2 Comparison of specific energy density of different battery types. a) Comparison of gravimetric energy density of LIBs and Li-S batteries (data taken from [20]). b) Comparison of volumetric and gravimetric energy density of Li-S and LIB (data taken from [21]).*

Since their first prototype in the 1960s, lithium-sulphur (Li-S) batteries have been viewed as a promising high-energy-density secondary battery system, which goes beyond conventional Lithium-ion batteries [20–22], see Figure 2. The theoretical energy density of Li-S batteries is above 2500 Wh kg<sup>-1</sup>, which is five times higher than that of commercially available LIBs [23]. It is widely estimated in the literature that energy densities beyond 500 Wh kg<sup>-1</sup> constitute a realistic goal for Li-S batteries [1,24,25]. This energy density would extend the driving range for an electrified vehicle up to 500 km [26]. Replacing the insertion-type cathode materials in LIBs with sulphur has several advantages. Many of the transition metal compounds used as cathode materials in LIBs are rare, expensive, and toxic. In contrast, the low-cost sulphur is one of the most abundant elements on earth, and is environmentally friendly [27]. This

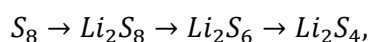


provides the Li-S battery technology with an economic and ecologic advantage and makes them also attractive for large-scale energy storage applications related to renewable energy sources, e.g., solar and wind. Furthermore, due to the two-electron conversion reaction per sulphur atom, sulphur has the highest theoretical capacity of 1675 mA h g<sup>-1</sup> among the solid elements. In addition, sulphur has a low operating voltage (2.15 V vs Li<sup>+</sup>/Li), which improves the safety [1].

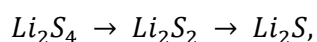
Typically, a Li-S battery consists of a metallic lithium anode, a sulphur cathode, an organic electrolyte and a separator, see Figure 3a) for an illustration [25]. The most used cathode material in Li-S batteries is elemental sulphur. Among the many sulphur allotropes, the ring-structural octasulphur S<sub>8</sub> is thermodynamically the most stable at room temperature. The working principle of Li-S batteries is conceptually different from the LIB technology, which is based on the intercalation of lithium into layered electrode materials. Instead of intercalation, the energy-storage mechanism of Li-S batteries relies on plating and stripping of metal on the lithium anode side, and a conversion reaction on the sulphur cathode side [21]. During the discharge process, at the negative lithium metal anode, Li-ions and electrons are formed via oxidation of the electrode, yielding the reaction



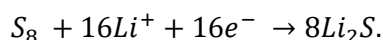
The Li-ions travel through the electrolyte towards the positive sulphur cathode, whereas the electrons move through the external circuit. Both, the Li-ions, and the electrons react at the sulphur cathode with sulphur, forming lithium sulphides (reduction). However, the lithiation of the sulphur is a complex multi-step process. First, lithiation of sulphur occurs via the formation of a series of intermediate, long-chain lithium polysulfide species (LiPSs) according to the sequence



These LiPSs with structure formula Li<sub>2</sub>S<sub>x</sub>, where 4 ≤ x ≤ 8, are primary discharge products at the cathode which dissolve into the electrolyte. Upon further lithiation, the dissolved long-chain polysulfides form insoluble short-chain sulphide species via



which re-precipitate onto the electrode as solid species. Hence, the final discharge product is Li<sub>2</sub>S. The conversion reaction between solid Li<sub>2</sub>S<sub>2</sub> and solid Li<sub>2</sub>S involves a much slower reaction kinetics than the first step of the sulphur-lithiation where the LiPSSs are formed. Altogether, during discharge this yields the reaction (at the sulphur cathode)



The two-step process explained above usually results in a two-plateau charge/discharge voltage profile which is typical for Li-S batteries [21]. Altogether, when discharging the Li-S battery, the corresponding electrochemical reactions reverse from solid S<sub>8</sub> to dissolved LiPSs to solid Li<sub>2</sub>S, such that Li-S batteries undergo a “solid-liquid-solid” phase transformation. This constitutes the “dissolution-precipitation pathway” for Li-S batteries. During charging the Li-S battery, the opposite reactions occur at the two electrodes (Li<sup>+</sup> + e<sup>-</sup> → Li at the negative electrode, and 8Li<sub>2</sub>S → S<sub>8</sub> + 16Li<sup>+</sup> + 16e<sup>-</sup> at the positive electrode), although the intermediate species may differ from those occurring during discharge.

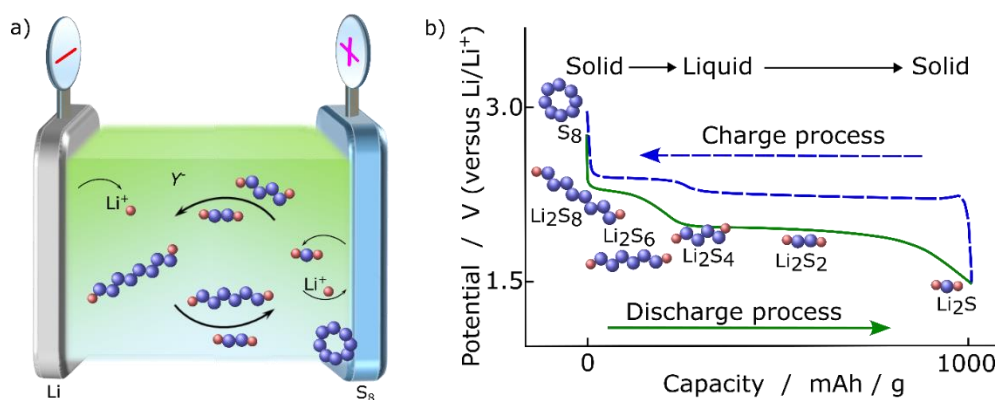


Figure 3 Illustration of the set-up and typical voltage profile of a Li-S battery. a) During discharge, Li-ions move towards the sulphur cathode, where lithium polysulfides form and move between the electrodes via a shuttle mechanism. b) Voltage profile for discharging / charging of a Li-S battery (data was taken from [1]).

However, despite the many promising aspects of Li-S batteries, there remain obstacles which prevent achieving the high theoretical capacity in real physical applications, and hinder future commercialization. These will be discussed in the two use cases, and a perspective will be presented on how to tackle them based on the objective of the EQUALITY project.

#### 4.2. Fuel Cells and The Solid Oxide Fuel Cell

Fuel cells (FCs) are electrochemical devices which transform chemical energy of a fuel and an oxidizing agent into electrical energy. The working principle is based on a pair of redox reactions. In contrast to batteries, FCs do not store energy, but require a continuous source of fuel and oxygen to provide electricity.

Fuel cells have been successfully commercialized for a wide range of mobile and stationary applications [28–30]. The stationary application of FCs includes small power devices of a few kilowatt (e.g., for households), up to megawatt-systems (e.g., energy backup in case of emergencies). In addition, there exists a long history of mobile applications. This includes the aerospace sector (e.g., in the NASA projects Gemini, Apollo or in the space shuttle program), but also aviation and fuel-cell cars.

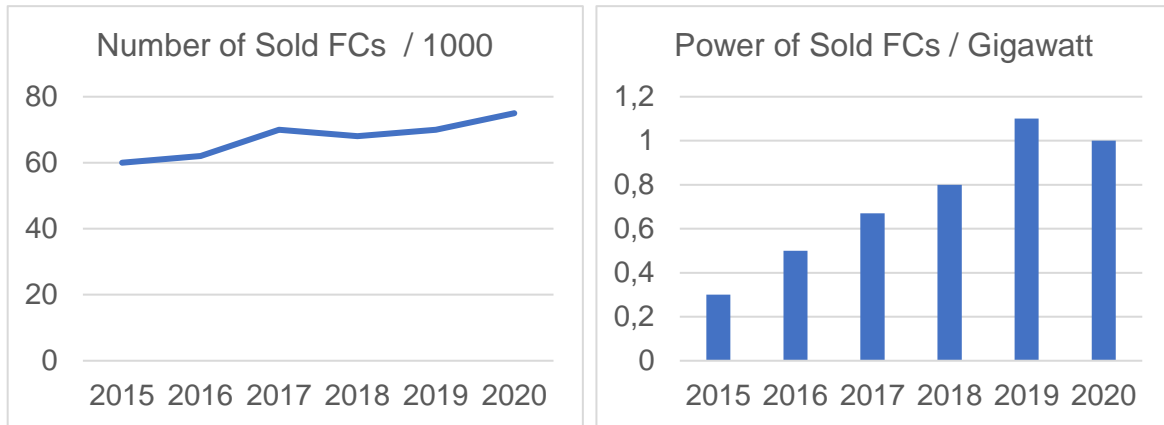


Figure 5 Market overview of FCs worldwide (source [41]).

However, there remain open problems for the development of better FC systems (e.g., increased fuel cell efficiency), or systems which allow for more convenient operating conditions (e.g., low-temperature solid oxide fuel cells, SOFCs).

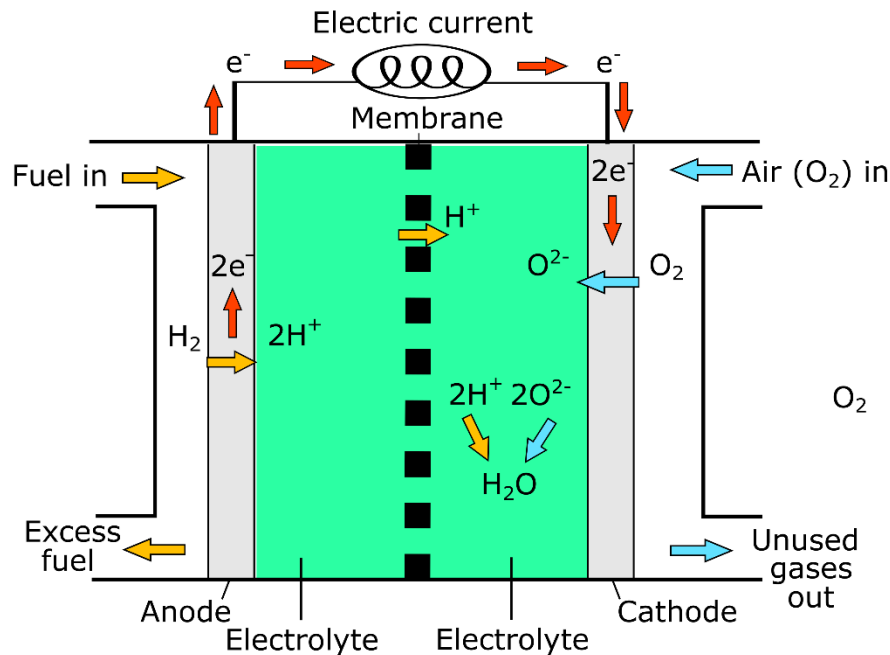


Figure 4 Illustration of the set-up of a SOFC.

There exist many different types of FCs, where the most prominent types are so-called proton-exchange membrane fuel cell (PEMFC), and the SOFC. However, they all rely on a common basic set-up, which consists of an anode, a cathode and an electrolyte. At the anode, the fuel undergoes an oxidation reaction which is caused by a catalyst. This produces positively charged ions, which are transported through the electrolyte towards the cathode. At the same time, electrons are conducted externally to the cathode via some electric circuit. This generates electric current which can be made use of. At the cathode, the ions are reduced as mediated by a catalyst, forming water. Often, the fuel consists of hydrogen and oxygen serves as oxidizing agent. Figure 4 illustrates the basic set-up of a FC via the example of a SOFC.

A detailed analysis of the various types of FCs lies beyond the scope of this document. However, for completeness, we here present a brief discussion of the SOFC.

### *Solid Oxide Fuel Cell (SOFC)*

The basic set-up of SOFCs was already discussed above, see also the illustration in Figure 4. SOFCs use solid oxides or ceramics as electrolytes, for example yttria-stabilized zirconia (YSZ). They operate on high temperatures to allow for an efficient transport of negative oxygen ions from the cathode to the anode through the electrolyte. The solid electrolyte is located between two electronically conducting electrodes, which are permeable for the gases. The side of the cathode which is not in contact with the solid electrolyte is surrounded by air, and the side of the anode which is not in contact with the solid electrolyte is surrounded by fuel gas. In FCs, the reduction and oxidation, which form the overall redox reaction, are spatially separated. In SOFCs, the redox reaction involves the reaction of oxygen with the fuel gas, typically hydrogen or some carbon monoxide. At the cathode side, there exists an excess of oxygen. In contrast, a shortage of oxygen exists at the anode where the oxygen reacts with hydrogen. This constitutes a concentration gradient of oxygen between the two electrodes and leads to diffusion of the oxygen ions from the cathode to the anode. In the presence of an electric current, these ions react catalytically with hydrogen ions at the anode. During these reactions, heat is produced.

## 5. Partial Differential Equation Solvers for Battery and Fuel Cell Design (First use case)

In this section, we define the first use case of this deliverable. This use case is defined by the continuum modelling of the two benchmark electrochemical systems discussed in section 0 (Li-S battery and SOFC). The continuum modelling of these two systems results in closed sets of partial (algebraic) differential equations.

### 5.1. Continuum Simulations of Lithium Sulphur Batteries

In this section, we focus on the lithium sulphur battery system. This type of battery has been chosen as benchmark battery system to be discussed in this use case.

#### 5.1.1. Problem scenario description

Here, we present a detailed description for the problem scenario related to the Li-S battery system. For a detailed introduction of this battery system, we refer to section 4.1 of this document.

Despite the promising characteristics of Li-S batteries (see section 4.1), there still exist some key challenges that need to be addressed for improving performance and for future commercialization. As it has been outlined by a seminal investigation by Manthiram et al, it is currently very challenging to achieve the theoretical capacity [31]. The list of major problems comprises the large sulphur expansion upon sulphur-lithiation, the low sulphur electrical conductivity, and the shuttle effect. Material specific problems can be attributed to both electrodes, but also to the shuttle-effect which involves the electrolyte.

The sulphur cathode undergoes large volume expansions (roughly 80%) during the lithiation of the sulphur, i.e., via the conversion reaction from  $S_8$  to  $Li_2S$ . This property can be attributed to the  $S_8$  having much higher density ( $2.07 \text{ g cm}^{-3}$ ) than the  $Li_2S$  ( $1.66 \text{ g cm}^{-3}$ ) [32]. This imposes severe mechanical strain on the cathode, which leads to the structural pulverization of the material and the detachment of sulphur from the electrode [33]. The detached sulphur is electronically not connected to the electrode, which results in a permanent capacity fade. One approach to preserve the structural integrity of the cathode is provide void space which accommodates the volume change. However, since this decreases the volumetric energy density, the porosity must satisfy a delicate balance between volumetric energy and performance [31]. In addition, the rate of electrochemical reactions occurring at the sulphur electrode are limited by the fact that sulphur and  $Li_2S$  (the end-product of the above-described lithiation of sulphur), are insulating for both the electrons and the ions. This hinders the reaction kinetics at the cathode during discharge and results in low utilization of active material constitutes a limited electrical conductivity. Also, the conversion reaction  $Li_2S_2$  to  $Li_2S$  involves a solid-solid process which happens much slower than the formation of the LiPSs (during the first step of the sulphur-lithiation), such that the LiPSs can hardly be completely reduced to  $Li_2S$ . Usually, in practical conditions, these obstacles are addressed by the incorporation of the sulphur in a conductive matrix [34]. However, this approach has the disadvantage that it lowers the specific capacity. Another key challenge arises from the so-called shuttle-effect, which has negative effects on Coulombic efficiency, and which promotes a fast capacity decay and high self-discharge rate [31]. This effect is mainly caused by the generation of the long-chained LiPSSs, which soluble in most common electrolytes used for Li-S batteries. During discharge, the long-chained LiPSSs are formed at the cathode, which leads to the build-up of a concentration gradient towards the anode. The resulting driving force leads to diffusion of the LiPSSs toward the metallic lithium anode, where the LiPSSs are reduced and form insoluble

$Li_2S$ . This leads to an irreversible loss of active material, and passivation of the anode. Also, the accumulation of PS in electrolyte causes considerable increases in viscosity. However, once the cell is charged, the long-chain LiPSs are partially reduced to form short-chain LiPSSs which migrate into the direction towards the cathode under the influence of the electric field. This shuttling deteriorates the charging efficiency of the battery and negatively affects the cathode via inhomogeneous distribution of insulating sulphur due to repetitive dissolution and redeposition. However, at the same time, the dissolution of LiPSs is crucial for the performance of the battery, as it ensures high sulphur utilization, via the production of “fresh” sulphur at the electrode surface, for reduction to sustain electron transport. This implies the delicate trade-off between high sulphur utilization and cycling stability must be ensured. Lithium metal anodes have a high specific capacity ( $3860 \text{ mAh g}^{-1}$ ), and low reduction potential ( $-3.04 \text{ V}$  versus a standard hydrogen electrode). This makes them ideal for batteries with high energy density. However, Li metal anodes are notoriously difficult to handle, due to various properties. The formation of lithium dendrites due to uneven distributions of current density on the surface, and a lithium-ion concentration gradient at the interface between the electrode and electrolyte, may lead to the occurrence of short-circuits. This causes severe safety concerns. The mechanical strain imposed upon the metal anode during repeated lithium plating / stripping leads to crack formation. This lowers the utilization rate of lithium because of the formation of “dead” lithium. The high reactivity of lithium yields the formation of an unstable SEI, which can crack upon cycling. This results in the irreversible consumption of active lithium. In addition, a passivation layer forms on the surface of the lithium anode, due to the formation of  $Li_2S$  during the shuttling of the LiPSs. This limits the cycling stability of the battery.

Thus, there exists a variety of problems occurring at different length scales, which hinder the practical application of Li-S batteries. This constitutes a problem landscape where each issue must be addressed individually. However, due to the strong couplings and interactions between the specific cell parts of the Li-S battery, emphasis must be put on a thorough understanding of how the compartmentalized solution-trials fit smoothly into the overall goal to improve the complete system. Here, modelling methodologies provide a viable tool for addressing this task. In particular, the problem set involves effects happening on microscopic scales, as well as effects occurring on macroscopic scales, thus covering several orders of magnitude. This motivates using a holistic approach based on a fully coupled framework which involves methods based on atomistic models, and continuum models. Via such an approach, the atomistic results can be consistently used to parameterize the continuum model and to clearly identify the relevant energy scales.

Altogether, the Li-S battery constitutes a very promising battery system, and is well-suited for a holistic, multiscale modelling approach based on the combination of atomistic and continuum methods.

### 5.1.2. Chosen methods

In this section, we give a detailed description of the chosen methods for the continuum modelling of Li-S batteries. First, we present a brief introduction into the methodology of continuum modelling. Second, we describe the framework of rational thermodynamics (RT), which we employ for our derivation of the continuum model for Li-S batteries. Third, we specify the resulting mathematical model and discuss different limiting cases. Finally, we explain our planned procedure for how to use methods based on quantum computing to solve the different systems of differential equations and obtain numerical results.

Typically, continuum models describe physical objects at mesoscopic length scale ( $\mu\text{m}$ -scale), or at the macroscopic length-scale (mm-scale). On such length scales, the molecular / atomistic origin of matter can be neglected (continuum hypothesis for liquids), and the system is described as a continuum using methods from non-equilibrium thermodynamics, coupled with elements from electromagnetic theory and mechanics. Furthermore, it is usually assumed that the typical length-scale of the system is much larger than the interactions between individual particles.

The continuum hypothesis for liquids applies to the description of physical systems on a mesoscopic or macroscopic scale and neglects the particle nature of the system. According to this description, all physical variables emerge from microscopic quantities via averaging techniques, thereby erasing microscopic discontinuities. This approach has the advantage that averaged quantities, *e.g.*, free energy, temperature, density, pressure, and velocity, can be assumed to vary continuously in space. For this purpose, one focuses on a representative volume element  $dV$  within the system. This volume element must be large enough such that statistical fluctuations do not result in macroscopic fluctuations of the averaged quantities, and, at the same time,  $dV$  must be small enough to capture macroscopic variations (*e.g.*, velocity or concentration gradients). Usually,  $dV$  takes size on the order of cubic microns which suffices for the modelling of bulk effects in batteries.

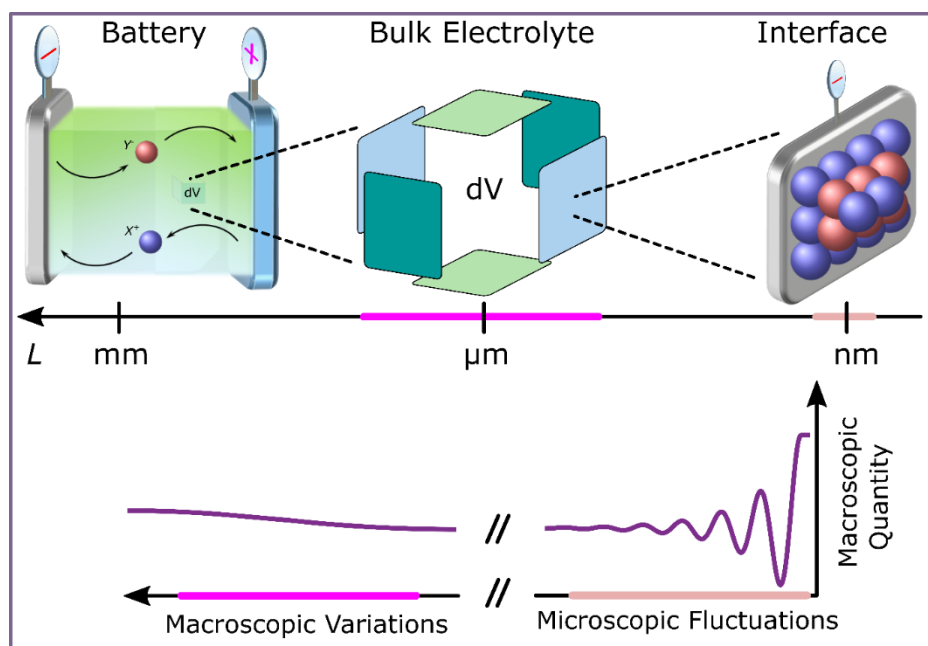


Figure 6 Illustration of the continuum hypothesis.

However, the continuum hypothesis is insufficient for the description of physical systems at length scales smaller than a few nanometers. Here, the typical length scales equal the size of the particles, and non-local particle interactions become dominant. Figure 6 illustrates the different scales of resolution, which can be applied for the modelling of a macroscopic system / battery. The continuum modelling of the bulk electrolyte focuses on the intermediate region of the length, whereas an enhanced resolution is mandatory for the description of microscopic effects, see the right region on the length bar. As an example, the lower part of this figure illustrates the profile for the ion-concentration of a macroscopic quantity on different length scales, *i.e.*, different scales of resolution. Typically, such profiles vary smoothly on the macroscopic scale, but exhibit fluctuations at the microscopic scale. For the derivation of our continuum model for Li-S batteries, we use the framework of RT [35,36]. RT is a description

of non-equilibrium thermodynamics, which puts emphasis on a rigorous physical foundation and consistency with the laws of thermodynamics. It is based on concepts of continuum mechanics, where universal balancing laws for energy, mass, momentum and charge provide a rigorous physical basis, which is kept separate from the specific material at hand. This approach has the advantage that it allows for the description of a large class of materials via one constitutive framework. When applied to a real physical system, the mutually coupled balancing laws are supplemented by material-dependent properties. Via the method of Coleman and Noll [37,38], this leads to case-specific constitutive equations which are derived from the Helmholtz free energy of the system. The free energy is the focal quantity in this constitutive modelling and determines the specific material representation. In addition, the thermodynamic fluxes are determined using an Onsager approach. However, RT also obeys important restrictions imposed upon the framework by universal arguments based on symmetry ("material frame indifference") and based on thermodynamic restrictions. Most importantly, they are restricted by the laws of thermodynamics ("thermodynamic consistency"), which are supposed to hold at any time. Thermodynamic consistency of the framework is implemented via the so-called entropy principle. Because all material specific properties are cast into the Helmholtz free energy, the framework provides a convenient tool for adjusting and modifying the material specific model. It is easily possible to increase the complexity of a model via a step-by-step approach based on modifying the free energy or adding additional contributions.

Below, we present a detailed analysis of the theoretical framework for the continuum description of Li-S batteries. This analysis is structured into three different parts, which apply to different regions of the electrolyte and are subject to differing simplifying assumptions. Our discussion explains the continuum theory for Li-S batteries and states the respective sets of transport equations. This analysis is still rather general, as we do not yet specify the model for the Helmholtz free energy of the system. However, once the Helmholtz free energy is specified, this determines the driving forces of the system and closes the equations of motion.

l) *Electrolyte Transport with Electrochemical Double Layer Formation*

The most general form of the framework yields a dynamical description of the system in the form of coupled transport equations for charge density  $\varrho$ , species concentrations  $c_\alpha$  and the volume-averaged convection velocity  $\mathbf{v}$  based on thermodynamic species fluxes  $\mathcal{N}_\alpha$  and the electric current  $\mathcal{J}$  [39–42]. For a system of  $N$  species in isothermal state, the evolution of the charge density and the species concentrations is determined by.

$$\begin{aligned} \frac{\partial}{\partial t} \varrho &= -\nabla \mathcal{J} - \nabla(\varrho \mathbf{v}) + \sum_{\alpha=1}^N F z_\alpha r_\alpha, \\ \frac{\partial}{\partial t} c_\alpha |_{\alpha \geq 3} &= -\nabla \mathcal{N}_\alpha - \nabla(c_\alpha \mathbf{v}) + r_\alpha, \end{aligned}$$

whereas the convection velocity is determined by a differential equation without time derivative

$$0 = \nabla \mathbf{v} - \sum_{\alpha=1} v_\alpha r_\alpha.$$

This set of transport equations must be supplemented by the Poisson equation, which couples the electric potential of the electrolyte ( $\Phi$ ) to the charge density,

$$\varrho = -\epsilon_0 \nabla(\epsilon_R \nabla \Phi).$$

Altogether, this constitutes a fully coupled set of algebraic differential equations (differential equations where time derivatives and space derivatives are coupled) and differential equations. In the set of equations above, reactions are comprised as source terms based on the specific reaction rates  $r_\alpha$ . Usually, these are modelled via a linear Ansatz  $r_\alpha = \sum_r v_r A_r i_r$ .



Here,  $A_\Gamma$  is the specific surface area of the interface labelled by  $\Gamma$ ,  $\nu_\Gamma$  is the stoichiometry of the reaction and  $i_\Gamma(\eta)$  is surface reaction rate. The surface reaction rate is a function of the overpotential  $\eta$  and can be determined via a Butler-Volmer Ansatz [43]. For the description of hardly compressible electrolytes, assuming the incompressible limit is usually a good approximation. This assumption allows to derive the above equation for the convection  $\mathbf{v} = \sum_{\alpha=1}^N \nu_\alpha c_\alpha \mathbf{v}_\alpha$  from the Euler property  $\sum_{\alpha=1}^N \nu_\alpha c_\alpha = 1$ , where  $\nu_\alpha$  are the partial molar volumes of the species, and  $\mathbf{v}_\alpha$  are the species velocities.

The thermodynamic fluxes comprise the transport mechanisms diffusion, migration and convection. For the species flux densities and for the density of the electric current, we find.

$$\mathcal{N}_\alpha = \frac{t_\alpha}{Fz_\alpha} \mathcal{J} - \sum_{\beta=3}^N D_{\alpha\beta} \nabla \mu_\beta,$$

$$\mathcal{J} = -\kappa \nabla \Phi - \kappa \sum_{\beta=3}^N \frac{t_\beta}{Fz_\beta} \nabla \mu_\beta.$$

These fluxes are functions of the transport parameters and the driving forces comprised in the gradients of the chemical potentials  $\nabla \mu_\beta$ . The set of independent transport parameters consists of N-3 transference numbers  $t_\beta$ ,  $N(N-3)/2+1$  independent diffusion coefficient  $D_{\alpha\beta}$  and the electric conductivity  $\kappa$ , and follows directly from the Onsager approach, whereas the driving forces are determined by the model for the Helmholtz free energy. In particular, the chemical potentials are given by a constitutive equation of the form  $\mu_\beta = \partial(\rho\phi_H)/\partial c_\beta$ .

We emphasize that only N-2 dynamical transport equations for the species concentrations are necessary. This is a direct consequence of the mutual couplings between the electrolyte species and of constraints thereon. However, the simplest description of electrolytes in Li-S batteries is to assume that they are composed of three species. In this case, the concentration of the lithium ions is chosen as the independent species concentrations,  $c_3 = c_{\text{Li}}$ . Furthermore, in addition to the transport equation for the charge density, there is one further transport equations for the lithium ions.

## II) *Electroneutral State: Bulk Electrolyte Transport*

However, for the description of the bulk electrolyte, it suffices to assume that the system is in electroneutral state such that  $\varrho = 0$ . Thus, the set of independent variables reduces to the species concentration  $c_{\text{Li}}$ , the electric potential  $\Phi$ , and the convection velocity  $\mathbf{v}$ . Furthermore, the Li-S battery employs porous cathode filled with liquid electrolyte. Thus, the transport equations must be modified using porous electrode theory [44–46].

In the bulk description where we assume electroneutrality, the set of independent variables reduces to the species concentration  $c_{\text{Li}}$ , the electric potential  $\Phi$ , and the convection velocity  $\mathbf{v}$ . Using porous electrode theory as described above, this leads to the following set of transport equations,

$$0 = \nabla \mathcal{J}^{\text{eff}} - \sum_{\alpha=1}^3 Fz_\alpha r_\alpha,$$

$$\frac{\partial}{\partial t} (\varepsilon c_{\text{Li}}) = -\nabla \mathcal{N}_{\text{Li}}^{\text{eff}} - \nabla(\varepsilon c_{\text{Li}} \mathbf{v}) + r_{\text{Li}},$$

$$0 = \nabla(\varepsilon \mathbf{v}) - \sum_{\alpha=1}^3 \nu_\alpha r_\alpha.$$

The effective species flux densities  $\mathcal{N}_\alpha^{\text{eff}}$  and the effective current density  $\mathcal{J}^{\text{eff}}$  are defined by.

$$\begin{aligned}\mathcal{N}_{\text{Li}}^{\text{eff}} &= \frac{t_{\text{Li}}}{F} \mathcal{J}^{\text{eff}} - \varepsilon^\beta D_{\text{Li}} \nabla \mu_{\text{Li}}, \\ \mathcal{J}^{\text{eff}} &= -\varepsilon^\beta \kappa \nabla \Phi - \varepsilon^\beta \kappa \frac{t_{\text{Li}}}{F} \nabla \mu_{\text{Li}}.\end{aligned}$$

Here,  $\varepsilon$  is the volume fraction of the electrolyte (“porosity”), and  $\beta$  is the Bruggemann coefficient which is related to the tortuosity of the electrode. The remaining dynamical transport equation for the lithium ions can be expressed via

$$\frac{\partial}{\partial t} (\varepsilon c_{\text{Li}}) = \sum_{\beta=1}^3 (\delta_\beta^{\text{Li}} - c_{\text{Li}} \nu_\beta - t_{\text{Li}} z_\beta) \cdot r_\beta - \frac{1}{F} \mathcal{J}^{\text{eff}} \cdot \nabla t_{\text{Li}} - \varepsilon \nabla (c_{\text{Li}}).$$

The first term on the right side (in brackets) can be simplified based on various assumptions. First, because the lithium is very small when compared with other typical ions and molecules present in an electrolyte, it is usually a good approximation to assume that  $c_{\text{Li}} \nu_{\text{Li}} \ll 1$ . Second, in many cases the transference numbers can be assumed constant. Third, among the electrolyte species, usually only the lithium participates in Faradaic reactions at the electrode. Because we apply these assumptions repeatedly throughout this document, we list them here:

- A 1 Constant transference numbers
- A 2 Only lithium participates in Faradaic reactions at the electrodes.
- A 3 The volume fraction of lithium species is very small,  $c_{\text{Li}} \nu_{\text{Li}} \ll 1$

Based on all these three assumptions, we find  $\nabla \mathcal{J}^{\text{eff}} = F r_{\text{Li}}$  and  $\nabla (\varepsilon \nu) = \nu_{\text{Li}} r_{\text{Li}}$  such that the transport equation of the lithium ions becomes,

$$\frac{\partial}{\partial t} (\varepsilon c_{\text{Li}}) = (1 - t_{\text{Li}}) \cdot \nabla \mathcal{J}^{\text{eff}} / F - \varepsilon \nabla (c_{\text{Li}}).$$

### III) *Electrolyte Description with LiPSs*

As described above, the formation of LiPSs during charging / discharging the cell constitutes a limiting factor for the performance of Li-S batteries. The LiPSs dissolve in the electrolyte and are transported throughout the cell via the shuttle effect. The influence of the shuttle effect on the overall cell performance can be captured in the modelling via incorporation of the LiPSs as individual electrolyte species. To address this goal, the set of transport equations must be supplemented by one additional transport equation per additional electrolyte species. Also, an increased number of electrolyte species must be taken account for in the number of electrolyte species which participate in reaction-source terms (appear in the transport equations).

According to our description of the electrolyte transport, the additional equations per additional electrolyte species take the form

$$\frac{\partial}{\partial t} (\varepsilon c_{\text{LiPS}}) = -\nabla \mathcal{N}_{\text{LiPS}}^{\text{eff}} - \nabla (\varepsilon c_{\text{LiPS}} \nu) + r_{\text{LiPS}}.$$

### IV) *Stationary Description of the EDL*

Experiments and theoretical arguments show that quasi-crystalline structures form at the electrode / electrolyte interface [41,47]. This constitutes the EDL, which plays an important role for the performance of a battery [48]. For the description of the electrochemical double layer, it suffices to consider the quasi-stationary description of the variables charge density  $\varrho$ , ion concentration  $c_{\text{Li}}$ , and electric potential  $\Phi$  (where the system is not assumed in electroneutral state) [49]. Using no-flux boundary conditions [39],

$$\nabla\mu_{Li} = 0,$$

$$\nabla\mu_{Y^-} = 0,$$

$$\varrho = -\epsilon_0 \nabla(\epsilon_R \nabla\Phi).$$

Here,  $\nabla\mu_{Y^-}$  is the driving force with respect to the anion-species resulting from the dissociation of the  $LiY$ -salt.

V) *Cell Modelling: Multiphase / Electrode Evolution*

The dissolution and formation of complex LiPSs occurring in Li-S batteries during discharging / charging described above has significant influence on the volume fraction of the bulk phases of the liquid electrolyte and of the bulk phase of the electrodes. The evolution of the phases can be accounted by the volume fractions  $\varepsilon_a$  of the two phases. Here,  $a \in \{l, s\}$ , where  $l$  denotes the liquid phase of the electrolyte and  $s$  denotes the solid electrode phase. By construction, the individual bulk phases are subject to the normalization constraint.

$$\sum_a \varepsilon_a = 1.$$

This, of course, just expresses the property that the available volume is always “filled” by some bulk phase. Because of the interface reactions, the volume fractions of the individual phases change with time. Mass conservation of reactions involving two phases can be described by [50],

$$\frac{\partial(\rho_a \varepsilon_a)}{\partial t} = M_\alpha r_\alpha \cdot A,$$

where  $A$  accounts for the volume specific surface area corresponding to the interface reaction,  $M_\alpha$  is the mean molar mass of the bulk phase, and  $\rho_\alpha$  its mass density. However, in the case where there is an additional gas phase present, e.g., in the case of fuel cells, mass conservation is better described via.

$$\frac{\partial(\rho_a \varepsilon_a)}{\partial t} = M_\alpha r_\alpha \cdot \ell / A.$$

Here, the active surface area is replaced by the active boundary length  $\ell$  between all involved phases.

*Modular Approach for the Numerical Solving of the Continuum Theory in the Case of the Li-S*

The above cases discussed in the paragraphs II) and III) comprise special cases of the theoretical description for Li-S batteries. They are variations of the general description presented in I), and must be supplemented by solid phase equations for the electrodes. In Table 3, we summarize the different descriptions and their areas of applicability.

Type	I)	II)	III)	IV)
Bulk	✓	✓	✓	X
EDL	✓	X	X	✓
Dynamical	✓	✓	✓	X

Table 3 Model Variations of the Continuum Description for Li-S batteries.

The simplest form for the solid phase equations is to set the electrode potential of the lithium metal anode to zero, use a Faradaic interface condition  $0 = I + F \int dx \sum_{\alpha} z_{\alpha} r_{\alpha}(U_{\text{cathode}})$  for the sulphur cathode. A more detailed description of the multiphase evolution then involves a description as presented in V).

Altogether, these model variations constitute the basis on which the quantum algorithms shall be applied and evaluated. To address this goal, we propose a modular approach, where the theoretical complexity of the description, which correlates with the numerical costs, increases stepwise. Our modular approach consists of three steps. The first step focuses on the simplest cell-description. The second and third step increase the complexity, culminating in the fourth step, which is the most general description. All simulations are performed in one spatial dimension and beginning with a limited number of grid points. Depending on the performance results, the numerical complexity can be adjusted by varying the number of grids points or increasing the dimensionality to 2D or 3D simulations. Next, we present a detailed description of the steps.

**Step 1 Description of ternary electrolyte:** The non-convective electrolyte is described in stationary state, as discussed in II). Solid phases are described by the simple solid phase equations presented above.

**Step 2 Incorporation of LiPSs:** The electrolyte description of step 1 is extended by accounting for an increased number of electrolyte species (LiPSs), see the discussion in III). Depending upon the progress and performance, this investigation will be extended to the dynamical description of the electrolyte.

**Step 3 Multiphase Evolution:** The electrolyte descriptions of the previous steps will be supplemented by the evolution of the phases as discussed in V).

In particular, the first step is to focus on the simplest theoretical description presented in II). As it was shown, this description assumes fast relaxation times, leading to stationary profiles of the macroscopic variables like the concentration of the lithium ions. Thereby, the dynamical description based on a complex set of algebraic differential equations reduces to simple diffusion equations. Diffusion equations have the advantage that they are much easier to solve numerically. In the beginning of each step, a rather coarse-grained numerical implementation for the calculations given by a limited number of grid points can be used. Based on the performance of the quantum algorithms, the number of grid points can then be adjusted to better evaluate limitations of the algorithm and identify deficiencies. Potential modifications shall be again evaluated for a limited number of grid points, eventually increasing them again. Once this yields satisfactory results, the next step will be tackled. Here, the same strategy will be applied.

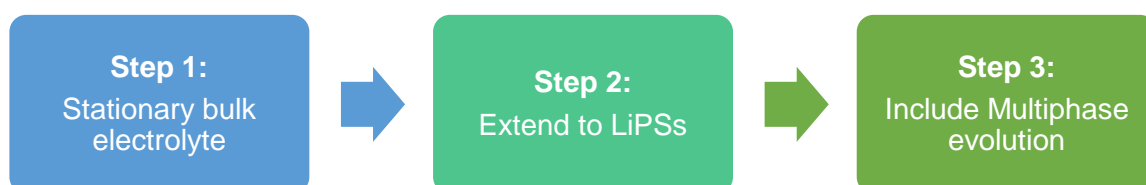


Figure 7 Modular set-up for the electroneutral cell simulations.

Optionally, based on the performance results in the as-described steps 1-3, a parallel investigation track can be tackled, which focuses on the description of the EDL at the interface between the electrode and electrolyte. The simplest theoretical description of the EDL is the

stationary approach presented in IV), whereas the dynamical description of the EDL which is numerically challenging was presented in I).

The overall goal is to combine both tracks and to enable the quantum algorithm to be applied to the description of the complete cell, which combines both the liquid bulk track and the electrode track into one framework.

### 5.1.3. Implications

Here, we discuss the implications of our activities outlined in section 5.1.2.

The successful implementation of quantum algorithms for solving differential equations would have significant implications for continuum modelling. It is to be expected that this would lead to a dramatic increase of computational power for performing numerical simulations based on the continuum models [51].

The increase in computational power for solving partial differential equations can be used to enhance the resolution of continuum models, while, at the same time, consider large systems [52,53]. This can be seen as follows. For a system of length  $L$ , the number of grid points  $N$  is defined by the step-size of the grid  $\Delta x$  via

$$N \sim \frac{L}{\Delta x}.$$

More computational power allows to use more grid points ( $N$ ) in the numerical simulations. According to the relation from above, this can either be achieved by increasing the length of the physical system ( $L$ ), yielding a larger system, or decreasing the step-size of the grid ( $\Delta x$ ), which enhances the resolution. However, the ideal scenario is that the computational power allows to implement both steps for numerical simulations of continuum models, *i.e.*, increasing the system and enhancing the resolution. Altogether, quantum algorithms may enable solving large systems on small scales allowing for the effective application of continuum models to real physical systems over several length scales. This is currently not a realistic scenario when classical computers are used. Also, it facilitates coupling continuum models to atomistic models via the direct parameterization of the continuum model using results of atomistic simulations. For batteries, one important application would be to study a complete cell using a resolution which incorporates double layer effects, thus coupling bulk and interfacial properties.

In addition to the properties that larger systems can be investigated, and that the resolution can be enhanced, increased computational power also leads to shortened run-time of numerical simulations. As consequence, very many numerical simulations can be performed in each time. A key advantage of continuum models is that they can be used very effectively for the evaluation of materials, or for the performance assessment of batteries when run in large cycles, *e.g.*, via a parameter screening. Therefore, shortened run-times are very beneficial for the application of continuum models and leads to a higher throughput of simulations. This constitutes a significant boost for the realistic application of continuum models to study physical systems. Eventually, this improves the potential of continuum models to successfully give design - / and material recommendations for the development of batteries.

Finally, both the above implications can also be used to correct or refine the continuum modelling for a given system. Usually, the continuum model for a given system is validated in comparison with experimental results. Alternatively, a continuum model can be evaluated in

comparison to well-known properties of a system. However, in both scenarios, fast and efficient numerical simulations lead to a speed-up of the validation process. This has positive implications on the modelling process and leads to a more efficient quality analysis of the theoretical model based on numerical results.

Altogether, the successful application of quantum algorithms to solving coupled systems of partial (algebraical) differential equations via numerical simulations has many significant implications. It allows for the simulations of large systems at small length scales and improves the process of model variations.

#### 5.1.4. Impact on stakeholders

In this section, we discuss the impact on the stakeholders. We divide our discussion into two parts. First, we focus on the impact of improved Li-S batteries on stakeholders. Second, we discuss the implications of solving partial (algebraical) differential equations using quantum algorithms on stakeholders.

Lithium sulphur batteries have long promised to be a transformative technology for the energy storage industry, offering higher energy densities, lower costs, and longer lifetimes than traditional lithium-ion batteries. However, the practical adoption of this technology has been hindered by several challenges, including poor cycle life, low power density, and the so-called "shuttle effect", which causes the dissolution of lithium polysulfides and compromises the stability of the battery. Nevertheless, recent advancements in material design and manufacturing processes have brought lithium sulphur batteries closer to commercialization, with the potential to drive innovation in various sectors, including the aerospace industry.

The aerospace industry is one of the primary beneficiaries of lithium sulphur batteries, as it relies heavily on energy-dense and lightweight power sources [24,54]. The main applications of batteries in aerospace include auxiliary power units (APUs), hybrid-electric propulsion systems, and energy storage for emergency situations. In addition, batteries are used for satellite and space missions, where the high specific energy of lithium sulphur batteries can significantly reduce the payload and launch costs of spacecraft.

The performance improvements in lithium sulphur batteries will enable the aerospace industry to achieve new levels of efficiency and sustainability while enhancing safety and reliability. For instance, the use of lithium sulphur batteries as APUs can reduce the weight and size of the system, which in turn reduces fuel consumption and carbon emissions. This is particularly important for aircraft, where weight reduction is a critical factor in improving fuel efficiency and range. In addition, high specific energy of lithium sulphur batteries can enable the development of electric aircraft with longer ranges and faster speeds, competing with the traditional combustion engines.

Another application of lithium sulphur batteries in the aerospace industry is for unmanned aerial vehicles (UAVs), also known as drones. UAVs require lightweight and high-performance batteries, as they need to carry various payloads or sensors while staying aloft for extended periods, often in hostile environments. The use of lithium sulphur batteries in UAVs can increase their endurance, range, and speed, while reducing their carbon footprint and noise pollution. In addition, the high specific energy of lithium sulphur batteries can enable the development of larger and more capable UAVs, such as those used for search and rescue, surveillance, and cargo delivery.

The commercialization of lithium sulphur batteries in the aerospace industry requires a robust supply chain and manufacturing infrastructure, as well as compliance with safety and

regulatory requirements. The production of high-quality and consistent lithium sulphur batteries involves several steps, such as electrode preparation, cathode synthesis, electrolyte formulation, and cell assembly. Furthermore, the recycling and disposal of lithium sulphur batteries need to be addressed to minimize their environmental impact and maximize their value.

Several companies and organizations are currently working on the development and deployment of lithium sulphur batteries in the aerospace industry. For example, Oxis Energy, a UK-based battery manufacturer, has demonstrated a lithium sulphur battery with an energy density of 400 Wh/kg, which is more than double that of conventional lithium ion batteries [55]. This battery has been tested in UAVs, and it shows promising results in terms of performance, safety, and cost-effectiveness. In addition, NASA has funded several research projects on lithium sulphur batteries, aiming to enhance their thermal stability, charge rate, and cycle life, as well as their compatibility with space missions [56].

The adoption of lithium sulphur batteries in aviation faces several challenges, including scepticism from traditional and risk-averse players, such as airlines and aircraft manufacturers, and regulatory barriers related to safety, reliability, and certification. These challenges can be overcome by a concerted effort from industry, academia, and governments, as well as by the demonstration of the practical benefits and feasibility of the technology. Furthermore, the development of standards, protocols, and certifications for lithium sulphur batteries can enhance the confidence and trust of stakeholders in the technology and accelerate its deployment in the aerospace industry.

Finally, we discuss the implication of using quantum algorithms for solving partial (algebraical) differential equations on stakeholders. Computer aided engineering (CAE) is used in many industrial applications, but also in fundamental science. The range of applicability includes stress analysis of material components based on finite-element methods, thermal and fluid analysis using computational fluid dynamics, and multibody dynamics. This constitutes a market demand for efficient and convenient software-solutions for the numerical simulation of systems of coupled differential equations (multi-physics problems). Currently, most of the commercially available software relies on classical computing concepts (e.g., COMSOL Multiphysics, OpenFOAM, and MATLAB). Therefore, the advent of efficient quantum software for solving such multi-physics problems implies a huge stimulus for the providers of CAE software.

## 5.2. Continuum Fuel Cells Simulations

In this section, we focus on fuel cells and put emphasis on the solid oxide fuel cell. This type of fuel cell has been chosen as benchmark system to be discussed in this use case.

### 5.2.1. Problem scenario description

Here, we present a detailed description for the problem scenario related to the solid oxide fuel cell. For a detailed introduction of this type of fuel cell, we refer to section 4.2 of this document.

Despite the promising characteristics of Li-S batteries (see section 5.1), there still exist some key challenges that need to be addressed for improving performance and for future commercialization.

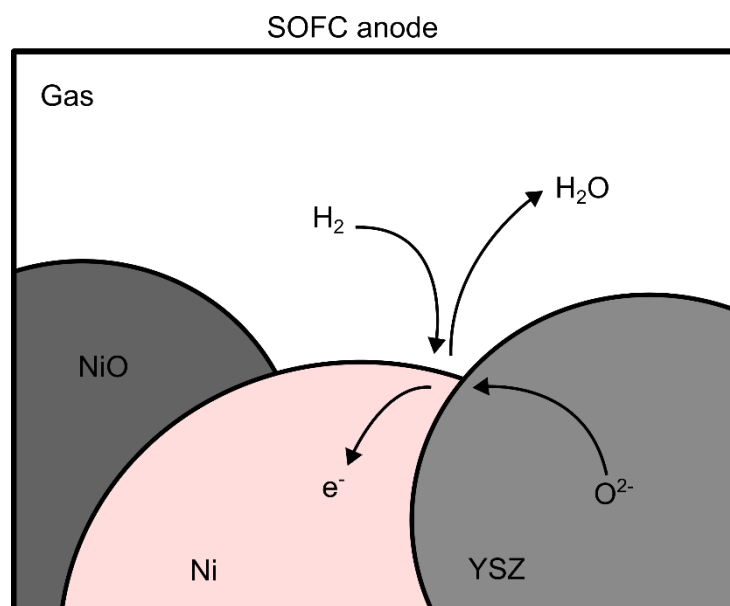
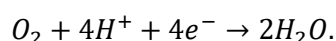


Figure 8 Illustration for the multi-phase reactions occurring at the SOFC anode.

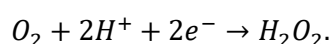
One common obstacle for achieving the goals outlined in section 4.2 can be attributed to the complex multi-phase environment which exists in FCs. FCs are characterized by the presence of multiple solid, liquid and gaseous phases, which are crucial for the cell functionality. We illustrate the multi-phase environment of SOFCs in Figure 8. The complexity of the system environment is increased by the multi-layer design. Typically, FCs consists of various components layers, including current collectors, electrode channels, electrodes, electrolyte, and separator. In addition, commercial applications often rely on stacked FCs where the air/fuel supply, the water management and the heat management play an important role. This highlights that an improved understanding, and an improved theoretical prediction of this multi-phase environment is crucial for the development of better FCs. Therefore, modelling of the systems plays a vital role for improving fuel cell technology.

#### Oxygen Reduction Reaction (ORR)

In this context, the ORR is a key process, which plays a vital role in FCs [57]. Developing a fundamental understanding of the ORR has attained much research interest in the last decades, as it facilitates the development of improved materials (e.g., the development of improved ORR catalysts). In FCs, the ORR is can be very slow, thus negatively affecting overall cell performance [58]. Basically, the ORR can evolve via two different reaction pathways. The first is that during the ORR, oxygen is reduced to two water molecules



Thereby, four protons and four electrons are transferred. The second one is a less efficient two-step two-electron pathway, in which hydrogen peroxide is formed in as an intermediate reaction product,



The four-electron pathway is preferable for achieving highly efficient FCs. This can be achieved by catalysts which increase the reaction times involved, thereby boosting the efficiency of the FCs. The most common catalysts are platinum and it's alloys [59], which have the disadvantage of being expensive. In addition, these catalyst materials suffer from CO



poisoning and from changes in the morphology of the catalyst layer, which limits their large-scale applications [60]. Currently, extensive research is being conducted to reduce or replace platinum-based electrodes in FCs [61]. Altogether, a fundamental understanding of the catalytic mechanism will provide guideline for increasing the efficiency of these catalysts and discovering new catalysts. The theoretical description and modelling of these systems can provide such understanding.

### 5.2.2. Chosen methods

In this section, we present a detailed description of our technical approach and describe the methods used to address the goals outlined above.

The electrolyte transport theory and the solid phase equations presented in section 5.1.2 are very general and describe a multitude of different system scenarios. They can be used for the continuum description of fuel cells. This statement is true for all the different variations of the transport equations, *i.e.*, with / without convection or stationary / dynamical. For this reason, we refer to section 5.1.2 for a comprehensive description of the corresponding set of transport equations.

However, due to the multiphase environment which is present in SOFCs, these transport equations must be supplemented by equations for the gas-phase transport in channels, as well as in the porous electrodes [50]. As another consequence of the multiphase environment, the evolution of the phases is of vital importance for SOFCs. Thus, the description of multiphase environment presented in the subcase V) in section 5.1.2 becomes mandatory for the SOFC model.

The continuum modelling of the oxygen reduction reaction (ORR) is usually performed via a mean field approach [57,62,63]. These allow to describe the surface coverage of the catalysts during the ORR via continuum equations. However, such mean field kinetics models rely on elementary parameters, like binding energies of reactants and intermediates on the catalyst surface. These parameters can be determined via atomistic modelling and validated with experiments. Therefore, the continuum model can be fully parametrized by the atomistic model, which highlights the relevance of the holistic approach which is presented in this document. However, in the case where high reaction rates are present, theoretical emphasis must be put on the influence of varying surface coverages on the catalytic activities [64]. The surface coverage  $\theta_j$  is defined by the product of the surface concentration of the respective species  $c_j^{\text{surf}}$ , the number of active surface sites  $\sigma_j$  occupied by the species  $j$  and the surface site density  $\Gamma_j$ ,

$$\theta_j = c_j^{\text{surf}} \sigma_j \Gamma_j.$$

In this description, it is assumed that large molecules occupy two surface sites, *e.g.*,  $O_2$  or  $HO_2$ , whereas smaller molecules occupy one surface site, *e.g.*,  $H_2O$  or  $HO$ . The dynamics of the surface coverage can be described via a mean field description

$$\frac{d\theta_j}{dt} = \sigma_j \sum_{i \in \text{reaction}} \nu_{i,j} \cdot \dot{s}_i.$$

Here,  $\nu_{i,j}$  denote the stoichiometric coefficients, and  $\dot{s}_i$  is the reaction rate. The correct thermodynamic description of the reaction rates is based on the evaluation of the mass action law via using the activities  $a_j$  (instead of concentrations) [65],

$$\dot{s}_i = k_i^f \prod_{j \in \text{educts}} a_j^{-\nu_{i,j}} - k_i^b \prod_{j \in \text{educts}} a_j^{\nu_{i,j}}.$$

The forward reaction rates  $k_i^f(A_i^{\text{f,act}}, U, \alpha_i)$  follow from on Arrhenius Ansatz [50,66] based on transition state theory, and are function of the activation energies  $A_i^{\text{f,act}}$ , the potential difference between the electrode and the electrolyte  $U$ , and the symmetry factors  $\alpha_i$ . The backward reaction rates  $k_i^b(k_i^f, \mu_i)$  can be determined from the forward reaction rates and the chemical potentials  $\mu_j = \mu_j^0 + \mu_j^{\text{int}}$  via the de Donder relations [57]. The chemical potentials  $\mu_j^{\text{int}}$  account for the interactions between surface adsorbents, and follow from the Gibbs free energy  $G^{\text{int}}$  for the interaction density via  $\mu_j^{\text{int}} = \partial G^{\text{int}} / \partial c_{j,\text{surf}}$ , where

$$G^{\text{int}} = \frac{n}{2} \sum_{jk} E_{jk}^{\text{int}} \cdot \frac{c_j^{\text{surf}} \cdot c_k^{\text{surf}}}{\Gamma_{\text{surf}}}.$$

Here,  $n$  is the coordination number which counts the number of nearest neighbours, and  $E_{jk}^{\text{int}}$  is the interaction energy between surface species  $j$  and  $k$ .

However, for many applications it suffices to consider the steady state of the system of algebraic equations [57]. This simplifies the description of the surface coverage, which becomes

$$0 = \sigma_j \sum_{i \in \text{reaction}} \nu_{i,j} \cdot \dot{s}_i.$$

The input parameters for the above discussed continuum description of the ORR, like the chemical potential and the interaction energies, can be determined by atomistic simulations, e.g. DFT calculations [67]. This highlights that the holistic modelling approach presented in this document yields a consistent and self-contained fully parametrized description for the ORR.

#### *Modular Approach for the Numerical Solving of the Continuum Theory in the Case of the SOFC*

For the case of the continuum description of the SOFC via the quantum approach, we use a modular approach which is like the approach described in section 4.1. However, because the multiphase environment is mandatory for the SOFC case (in contrast to the Li-S system), we slightly modify the modular approach of the Li-S case and define the following steps.

**Step 1 Cell model** Transport processes are described in stationary state, where convective effects are neglected, as discussed in case II) of section 5.1.2.

**Step 2 Elementary kinetics** The elementary kinetics of the ORR is modelled in agreement with the cell model based on quantum chemical data (see use case 2 described in section 6).

In particular, the first step is to focus on the simplest theoretical description of the SOFC, including the description of the multiphase environment. In step 2, we focus on the modelling of the ORR as described in section 5.2.1. Optionally, the complexity can be increased further by incorporating the cell model from step one. Similar to our modular approach described in section 5.1.2, a limited number of grid points can be used in the beginning of each step. Based on the performance of the quantum algorithms, the number of grid points can then be increased. This allows a convenient evaluation of the limitations and deficiencies of the quantum algorithm.

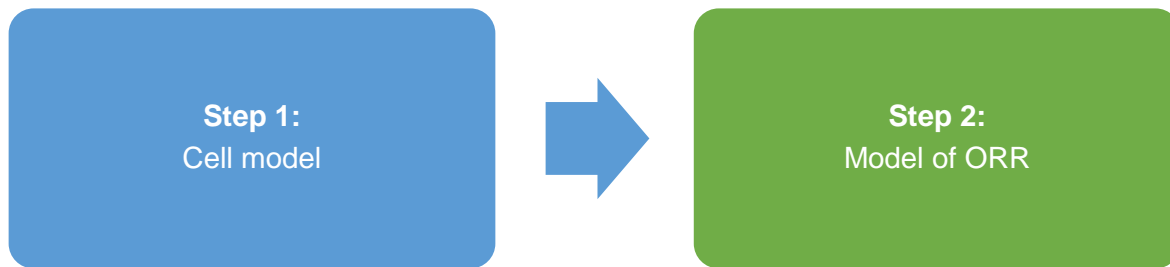


Figure 9 Modular approach for the Modelling of the SOFC.

### 5.2.3. Implications

In this section, we discuss the implications resulting from a successful implementation of the modelling activities for the SOFC described in section 5.2.2.

However, the continuum descriptions for Li-S batteries, as described in section 5.1.2, and for SOFCs, described in section 5.2.2, consist of almost exactly the same set of (algebraic) partial differential equations. Thus, both theoretical descriptions are rather similar. Consequently, the implications that would result from the successful implementation of quantum software for solving differential equations of continuum models, which have already been outlined in great detail in section 5.1.3, apply here as well.

However, for the completeness, we shortly repeat the main arguments here, and refer to section 5.1.3 for more details.

The main implication would result from the massive increase in computational power. In principle, this feature can be harvested in two ways. First, it can be used to increase the number of grid points, yielding allowing for the description of larger systems and for refining the resolution. Thereby, the simulations can account for more realistic results and for a multi-scale resolution. Second, the increase in computational power can be used to decrease the run-time of simulations, which allows for a high throughput of material / parameter screenings. Also, it allows for fast simulation-based feedback validation in the process of model variations, which makes the modelling effort more efficient.

Altogether, the above-described implications constitute a significant improvement for the simulation-based modelling activities of fuel cells.

### 5.2.4. Impact on stakeholders

In this section, we discuss the impact of a successful implementation of the modelling activities outlined in section 5.2.2 on the stakeholders. Like our discussion in section 5.1.4, this topic consists of two main parts. The first part deals with the impact on commercial providers of simulation software for continuum modelling, which would result from the ability to solve coupled sets of differential equations using quantum algorithms. The second part consists of the impact on research and development of SOFCs that would result from a quantum-based modelling approach.

Because the continuum descriptions of Li-S batteries and SOFCs are rather similar, the first aspect has already been addressed extensively in section 5.1.4. However, for completeness, we quickly repeat the main topics here. The commercialization of quantum software for solving coupled sets of differential equations would affect many providers of software related to computer aided engineering. Because the area of applicability of such simulation tools is very

large, including condensed matter physics, mechanics, biological and chemical physics, and engineering, the respective market for quantum-based simulation tools is also very large.

Finally, we discuss the impact of the successful implementation of quantum-based software for solving differential equations on the research and development of SOFCs.

As we have discussed in sections 5.1.3 and 5.2.3, the use of quantum-based software for solving differential equations would dramatically increase the computational power for performing continuum simulations. The resulting ability to conduct highly resolved multi-scale continuum simulations constitutes a significant improvement of SOFC-related research activities. The high resolution allows to account for microscopic effects, *e.g.*, reaction kinetics or interfacial properties, within simulations of macroscopic systems on cell level, which account for bulk effects, *e.g.*, transport. This helps improving the quality of the research, and, also, enhances the efficiency of conducting research.

In addition, the impacts resulting from using of quantum-based software for solving differential equations also apply to the development of better / novel types of SOFCs. The ability to conduct highly efficient computer screenings of materials and parameters related to SOFCs has significant impact on the ability to provide simulation-based recommendations for the design and materials used in the SOFC. This makes the development of SOFCs more efficient. On one hand, it provides the possibility to replace time-consuming and cost intensive experiments by computer simulations. Furthermore, there exist many aspects of the SOFC system, or specific components of the SOFC, which are hard to examine using experiments, but can be studied from a theoretical perspective. As consequence, an increase in the simulation-based abilities to tackle complex aspects of a given physical system automatically enlarges the portfolio of effects that can be studied. This may lead to technological solutions which would eventually not be considered without quantum-software.

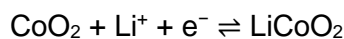
## 6. Solid Oxide Fuel Cell Optimization and Battery Material Discovery (second and sixth use case)

### 6.1. Materials discovery for battery design

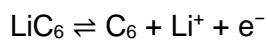
#### 6.1.1. Problem scenario description

Energy storage plays a crucial role in the transition towards renewable energy sources and sustainable development. LIBs have emerged as the dominant technology for energy storage due to their high energy density (up to 250 Wh/kg), no memory effect, long cycle life, and low self-discharge rates. Modern society relies heavily on LIBs, which are widely used in devices such as laptops, mobile phones, and electric vehicles.

Most commercial LIBs use intercalation compounds as the electrode material of choice. The anode of LIBs typically consists of carbon-based materials like graphite, while the cathode utilizes various metal oxides, such as lithium cobalt oxide (LiCoO<sub>2</sub>), lithium iron phosphate (LiFePO<sub>4</sub>), and lithium nickel manganese cobalt oxide (NMC). Separators are commonly made from different polymers, and electrolyte solutions often feature lithium salts dissolved in organic carbonates. During the battery's discharge process, the cathode functions as an oxidizing agent, which accepts electrons and undergoes reduction:



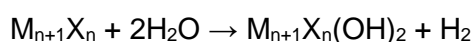
Conversely, the anode serves as a reducing agent, which donates electrons and experiences oxidation:

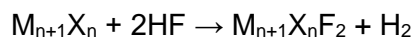


During the charging process, the reverse reactions occur (from right to left). At the cathode, LiCoO<sub>2</sub> releases Li<sup>+</sup> ions and electrons to become CoO<sub>2</sub>, while at the anode, C<sub>6</sub> accepts Li<sup>+</sup> ions and electrons to form LiC<sub>6</sub>. These electrochemical reactions enable LIBs to store and release energy as needed.

To further enhance the performance of LIBs, there is a growing interest in novel materials, particularly two-dimensional (2D) materials. These 2D materials offer unique advantages such as high specific surface areas, which provide numerous electrochemically active sites for ion storage, and open 2D channels for rapid ion transport [68]. In addition, their inherent mechanical flexibility and van der Waals bonding allow for seamless integration with existing active materials, resulting in improved LIB cell performance. With their diverse properties, 2D materials have the potential to impact every aspect of LIBs. For instance, hexagonal boron nitride (hBN) shows promise in separator and electrolyte applications [69]. Graphene analogs and transition metal dichalcogenides (TMDs) have been studied for their potential as anodes. [70] MXenes, which are composed of transition metal carbides and nitrides, has been widely investigated as LIB cathodes [71].

MXenes are a new class of two-dimensional materials first reported in 2012 [71]. Due to good electronic conductivity, fast Li diffusion, low operating voltage, and high theoretical Li storage capacity, MXenes are a promising anode material for LIBs. The synthesis of MXenes involves chemical reactions that selectively etch the "A" element from the MAX phase precursors. The general chemical reactions for the etching process are as follows:





In these reactions, "M" represents an early transition metal, "A" is an A-group element (mostly groups 13 and 14), "X" is C and/or N, and n is equal to 1, 2, or 3. The synthesis process results in the formation of functional groups, such as hydroxyl (OH) and/or fluorine (F), on the MXene surfaces, which can influence their properties and potential applications. For example, the  $Ti_3C_2$  monolayer exhibits magnetic metallic behaviour, while its derivatives,  $Ti_3C_2(OH)_2$  and  $Ti_3C_2F_2$ , are semiconductors with small band gaps [72]. The surface functionalization of F and OH impedes Li transport and reduces Li storage capacity, which should be avoided in experiments.

At present, more than 40 MXene compositions have been identified experimentally [73]. However, this number is anticipated to grow significantly in the future, leading MXenes to become the most extensive family of 2D materials known. Considering the great potential of MXenes and their diverse applications, exploring and discovering new MXenes using computational methods is a promising research direction. Computational screening facilitates the development of innovative materials and devices, expanding the scope and impact of 2D materials.

Exploring suitable 2D materials for LIBs through trial and error is time-consuming and inefficient. To extend the list of potential candidates, a 2D material identification theory and high-throughput screening methods are needed. Recently, [74] Song et al. proposed a usability identification framework, which leverages the competitive mechanism between the adsorbability and reversibility of ions on a 2D material, helping to screen practicable 2D materials more effectively. Additionally, they utilized density functional theory (DFT) calculations to verify the screened candidates and evaluate their battery performance. Their works not only significantly expand the available 2D materials for various battery demands but also provides a general methodology to assess the usability of unexplored 2D materials for LIBs [74].

Compared to classical computation, quantum computers offer unique capabilities in the field of materials design. These advanced machines can natively represent and manipulate quantum states, allowing for more efficient simulation of complex chemical systems. On a classical computer, the exponential growth of the dimension of the wave function makes manipulation and storage very inefficient. Although quantum computers are still in development and have not yet surpassed classical computers in all aspects, they hold great promise for quantum chemistry simulations in the future. By combining classical screening methods with the benefits of quantum computing, the process of discovering practicable 2D materials for battery applications can be significantly streamlined.

Li-S batteries have emerged as a potential alternative to LIBs, mainly due to their superior energy storage capabilities. As we have discussed in detail in section 4.1, the fundamental difference between Li-S and Li-ion batteries lies in their respective energy storage mechanisms. LIBs rely on the intercalation of lithium ions into layered electrode materials, while Li-S batteries operate based on metal plating and stripping on the lithium anode side and a conversion reaction on the sulphur cathode side. This non-topotactic nature of these reactions results in lithium anodes and sulphur cathodes having high theoretical specific capacities, providing Li-S batteries with a substantially higher theoretical energy density than LIBs (2500 vs. 250 Wh/kg) [21]. In addition to a high energy density, Li-S batteries are also cheaper due to the abundance and low cost of sulphur. This makes Li-S batteries an attractive and cost-effective energy storage technology. Li-S batteries have potential applications in various industries, including electric vehicles, renewable energy storage, and portable electronics.

Despite the potential of Li-S batteries, their widespread adoption is impeded by several limitations, including short cycling life, limited sulphur loading, severe polysulfide shuttling, and low sulphur utilization. One of the most critical issues is the shuttle effect, which results in rapid capacity fading and battery failure. The shuttle effect can be classified into five steps: (i) formation of long-chain polysulfides, (ii) detaching of polysulfides from the sulphur host, (iii) dissolution of polysulfides into the electrolyte, (iv) migration of polysulfides toward the lithium anode side, and (v) reaction between polysulfides and lithium anode [75]. To reduce the shuttle effect, researchers have focused on designing and fabricating sulphur host cathodes [76]. Initial efforts involved spatial encapsulation of sulphur by porous nanostructured sulphur hosts to suppress the diffusion of lithium polysulfides. This approach aimed to retain the polysulfides in the pores, preventing them from reaching the lithium anode. However, spatial encapsulation alone was not sufficient to fully address the shuttle effect. Therefore, researchers began developing sulphur host materials with strong chemical binding for lithium polysulfides. One such promising class of materials is MXenes, which have been experimentally demonstrated to be excellent Li-S battery hosts due to their high electrical conductivity and highly active 2D surfaces that can chemically bond intermediate polysulfides via metal-sulphur interactions [77].

DFT calculations have been employed to address the challenges associated with Li-S batteries, particularly the dissolution of intermediate lithium polysulfide ( $\text{Li}_2\text{S}_n$ ) species into the electrolyte. Anchoring materials that exhibit strong binding interactions with  $\text{Li}_2\text{S}_n$  species have been shown to be an effective way to overcome this issue and enhance long-term cycling stability and high-rate performance. By using first-principles approaches, including van der Waals interactions, Zhang et al. systematically investigated the adsorption of  $\text{Li}_2\text{S}_n$  species on various two-dimensional layered materials [78], such as oxides, sulphides, and chlorides. These investigations help to understand the binding strength, configuration distortion, and charge transfer at the atomic level, revealing the mechanisms behind the anchoring effect and identifying ideal anchoring materials to improve Li-S battery performance [78]. DFT calculations provide microscopic insight into the interaction features between anchoring materials and  $\text{Li}_2\text{S}_n$  species, leading to a more rational design of the cathode.

### 6.1.2. Chosen Methods

In this section, we elaborate on the chosen methods for atomistic simulations employed in battery material discovery and fuel cell simulation. First, we introduce the methodology of atomistic simulations, focusing on DFT, which provides a detailed understanding of materials and processes at the microscopic scale. In the second part, we discuss the use of DFT in combination with other computational methods to study the electrochemical reactions in Li-S batteries. In the third part, we will explore novel 2D materials with enhanced performance for batteries.

#### *Introduction of the methodology of atomistic simulations*

Atomistic simulations serve as a powerful tool for investigating materials and processes by explicitly accounting for the interactions between individual atoms and molecules. These simulations are particularly beneficial for studying systems where the particle nature of matter becomes dominant, typically at length scales smaller than a few nanometres. In such cases, the continuum assumption is insufficient, and atomistic simulations based on DFT are considered as an alternative. The outcomes of atomistic simulations can provide detailed insights into atomic and molecular interactions, electronic properties, and structural dynamics, which can help guide the design and optimization of materials for various applications, including batteries and SOFCs. Our simulations are mainly based on the ab initio approaches

using DFT, which does not rely on empirical parameters or fitting to experimental data. In this situation, atomic simulations can provide the necessary input data for continuum modelling, such as kinetic and thermodynamic data. Moreover, ab initio DFT calculations also allow for more accurate predictions of material properties and electrochemical reactions. Compared to experimental methods, atomistic simulations offer advantages such as reduced cost, easily control of system parameters, and the ability to study systems that may be challenging to explore experimentally.

DFT is based on the Hohenberg-Kohn (HK) theorems, which establish that the ground state energy of a system can be uniquely determined by its electron density and that the ground state energy is a functional of the electron density, with the minimum value corresponding to the true ground state electron density. Based on the HK theorems, the energy functional  $E[n(\mathbf{r})]$  can be expressed as

$$E[n(\mathbf{r})] = T_e[n(\mathbf{r})] + V_{Ne}[n(\mathbf{r})] + U_{ee}[n(\mathbf{r})]$$

where  $V_{Ne}[n(\mathbf{r})]$  is the functional of the potential energy between the electron and nuclei, which depends on the system under study

$$V_{Ne}[n(\mathbf{r})] = \int V(\mathbf{r})n(\mathbf{r})d^3r$$

Here,  $T_e[n(\mathbf{r})]$  and  $U_{ee}[n(\mathbf{r})]$  are functionals that define the electron kinetic energy and the electron-electron interactions, respectively. However, the explicit form of both functionals is still unknown. Kohn and Sham (KS) proposed a fictitious system consisting of non-interacting electrons, which move in a local effective potential  $V_s(\mathbf{r})$ . The KS equation has the following form

$$\left[ -\frac{\hbar^2}{2m_i}\nabla^2 + V_s(\mathbf{r}) \right] \phi_i(\mathbf{r}) = \epsilon_i \phi_i(\mathbf{r})$$

where  $\phi_i(\mathbf{r})$  is the KS orbitals that reproduce the electron density of the original interacting system, and  $\epsilon_i$  is the corresponding orbital energies. The effective potential  $V_s(\mathbf{r})$  can be written in more detail as

$$V_s(\mathbf{r}) = V(\mathbf{r}) + e^2 \int \frac{n(\mathbf{r}')}{|\mathbf{r} - \mathbf{r}'|} d^3r' + V_{XC}(\mathbf{r})$$

where the second term is the Hartree potential that describes the Coulomb repulsion between the electrons.  $V_{XC}(\mathbf{r})$  is the exchange-correlation term, which includes all the many-particle interactions

$$V_{XC}(\mathbf{r}) = \frac{\delta E_{XC}[n(\mathbf{r})]}{\delta n(\mathbf{r})}$$

Now, the complex many-body problem has been transformed into an effective single-particle problem, which is computationally much more feasible. However, the true form of the exchange correlation functional  $E_{XC}$  is simply not known. Finding good approximations for this functional is the main challenge of DFT. One of the most widely used approximations is the generalized gradient approximation (GGA), which improves upon the local spin density approximation (LSDA) by taking the gradient of the density into account



$$E_{XC}^{GGA}[n] = \int n(\mathbf{r}) \varepsilon_{XC}^{unif}[n(\mathbf{r})] F_{XC}[s(\mathbf{r})] d^3r$$

where  $\varepsilon_{XC}^{unif}[n(\mathbf{r})]$  is the exchange energy density of a uniform electron gas,  $s(\mathbf{r})$  is the dimensionless density gradient

$$s(\mathbf{r}) = \frac{|\nabla n(\mathbf{r})|}{2(3\pi^2)^{1/3}n(\mathbf{r})^{4/3}}$$

and  $F_{XC}[s(\mathbf{r})]$  is the enhancement factor for the given GGA. For example, in the popular Perdew-Burke-Ernzerhof (PBE) exchange functional,[79]  $F_{XC}$  has the following form

$$F_{XC}[s(\mathbf{r})] = 1 + \kappa - \kappa / (1 + \frac{\mu s^2}{\kappa})$$

where  $\kappa$  and  $\mu$  are (non-empirical) parameters determined by imposing certain physical constraints.

Usually, very good results for geometries and ground-state energies of solids can be obtained by using GGA. However, GGA does not describe van der Waals (vdW) forces well due to its “semi-local” nature, which is inadequate for capturing long-range interactions. To address this limitation, the D3 correction as proposed by Grimme and co-workers can be employed.[80] The general form for the dispersion energy is

$$E_{disp}^{DFT-D} = -\frac{1}{2} \sum_{A \neq B} \sum_{n=6,8,10,\dots} s_n \frac{C_n^{AB}}{R_{AB}^n} f_{damp}(R_{AB})$$

Here, the sum is over all atom pairs in the system,  $C_n^{AB}$  denotes the  $n$ th-order dispersion coefficient for atom pair AB, and  $R_{AB}$  is their interatomic distance. Scaling factors  $s_n$  can be used to adjust the correction to the repulsive behavior of the chosen exchange-correlation density functional.  $f_{damp}$  is a damping function to avoid overcorrection at short distances. The D3 correction enhances the accuracy of the DFT functional in describing van der Waals interactions, making it more suitable for systems where these forces are significant.

Another limitation of GGA functionals is their inadequate performance in predicting the electronic structure and energetics of systems with strong electron correlation effects. To overcome these limitations, hybrid functionals are used, which combine the exchange-correlation energy from GGA or LSDA with a fraction of the exact exchange energy from the Hartree-Fock (HF) theory. This mixture allows for better treatment of electron correlation effects, leading to improved accuracy in predicting molecular and solid-state properties. One of the most commonly used hybrid functional is B3LYP [81], which is expressed as follows

$$E_{XC}^{B3LYP} = (1 - a)E_X^{LSDA} + aE_X^{HF} + bE_X^{B88} + (1 - c)E_C^{LSDA} + cE_C^{LYP}$$

where  $E_X^{LSDA}$  and  $E_X^{B88}$  are both the exchange terms calculated in LSDA and Becke's GGA [82], respectively. Similarly,  $E_C^{LSDA}$  and  $E_C^{LYP}$  correspond to LSDA and Lee-Yang-Parr correlation functionals [83], respectively.  $E_X^{HF}$  is the HF exchange energy. The three empirical parameters in B3LYP were chosen to optimally reproduce the atomization, ionization, and protonation energies of molecules in the G2 database. These parameters are  $a = 0.20$ ,  $b = 0.72$ , and  $c = 0.81$ . These parameters help balance the contributions of various terms in the

B3LYP equation, facilitating error cancellation as closely as possible. The B3LYP functional has been shown to provide improved accuracy compared to GGA functionals like PBE for a wide range of molecular and solid-state properties. However, B3LYP is computationally more expensive, making it better suited for molecular systems and relatively small crystals.

Considering the limitations of DFT, particularly in handling strong electron correlation effects and van der Waals forces, more advanced quantum chemistry methods become necessary to achieve higher accuracy. One such method is the coupled cluster with single and double excitations plus a perturbative correction for triples (CCSD(T)), which often serves as a benchmark for evaluating the DFT results. The CCSD(T) has demonstrated its reliability across various applications and is typically capable of achieving chemical accuracy (within 1 kcal/mol) for electronic energies. However, as the molecular size increases, the computational cost of CCSD(T) grows dramatically, making it feasible only for benchmark studies on very small systems. To overcome this limitation, the domain-based local pair natural orbital method, DLPNO-CCSD(T), has been developed recently [84]. This technique retains the accuracy and reliability of CCSD(T) while enabling the calculation of systems with thousands of basis functions. Notably, DLPNO-CCSD(T) can recover 99.9% of the CCSD(T) correlation energy and can be considered as an alternative to quantum chemistry benchmarks.

The total DLPNO-CCSD(T) energy can be expressed as a sum of reference and correlation energies  $E_{\text{DLPNO}} = E_{\text{ref}} + E_{\text{C}}$  [85]. In the case of closed-shell systems, the reference determinant is typically the HF determinant, and hence,  $E_{\text{ref}}$  corresponds to the  $E_{\text{HF}}$  energy. For open-shell systems,  $E_{\text{ref}}$  is the energy of a high-spin open-shell single determinantal function, consisting of a single set of molecular orbitals. In the DLPNO scheme, electron pairs are classified as either "strong pairs", which contribute significantly to the correlation energy, or "weak pairs", which have negligible contributions. Such classification is based on the local second-order many-body perturbation theory. Strong pairs are treated at the coupled cluster level, while weak pairs are treated using a simpler second-order perturbation theory. The overall correlation energy is then obtained by summing the energies from strong pairs ( $E_{\text{C-SP}}$ ), weak pairs ( $E_{\text{C-WP}}$ ), and the perturbative triples correction ( $E_{\text{C-(T)}}$ ),

$$E_{\text{C}} = E_{\text{C-SP}} + E_{\text{C-WP}} + E_{\text{C-(T)}}.$$

This approach allows the DLPNO-CCSD(T) method to maintain high accuracy while significantly reducing the computational cost compared to traditional CCSD(T) calculations. For more details, we refer to the literatures [85].

#### *Atomistic simulations of electrochemical reactions in Li-S batteries*

First, we will focus on the atomistic simulation of electrochemical reactions occurring on the sulphur cathode, specifically, the stepwise reduction of sulphur to lithium sulphide through a series of intermediate polysulfide species. The overall electrochemical reaction can be represented as  $\text{S}_8 + 16\text{Li}^+ + 16\text{e}^- \rightarrow 8\text{Li}_2\text{S}$ . The B3LYP-D3 functional and cluster models will be used to optimize the geometries of reactants and products for each reaction step:  $\text{S}_8 \rightarrow \text{Li}_2\text{S}_8 \rightarrow \text{Li}_2\text{S}_6 \rightarrow \text{Li}_2\text{S}_4 \rightarrow \text{Li}_2\text{S}_2 \rightarrow \text{Li}_2\text{S}$ . Following the DFT calculations, we will employ the DLPNO-CCSD(T) method to obtain highly accurate single-point energies for the optimized structures. The Gibbs free energy of the species  $i$  at a given temperature is calculated as

$$G_i(T) = E_i + \Delta H_i(T) - TS_i(T)$$

where  $E_i$ ,  $\Delta H_i(T)$ , and  $S_i(T)$  are the single-point electronic energy, enthalpy change, and entropy, respectively.  $\Delta H_i(T)$  and  $S_i(T)$  are computed using the ab initio thermodynamic approach as follows

$$\Delta H_i = E_{\text{ZPE}} + k_B T \left( \frac{T}{q_v} \frac{\partial q_v}{\partial T} + 1 \right)$$

$$S_i(T) = k_B \left[ \ln(q_v) + T \frac{\partial \ln(q_v)}{\partial T} + 1 \right]$$

where  $E_{\text{ZPE}}$  is the zero-point energy,  $q_v$  is the vibrational partition function, and  $k_B$  is the Boltzmann constant, respectively.

To determine the free energy of  $\text{Li}^+ + \text{e}^-$ , we use the  $\text{Li}/\text{Li}^+$  electrode potential as the reference, which is chosen due to the Li metal anode utilized in Li-S batteries. This implies that the reaction  $\text{Li} \rightarrow \text{Li}^+ + \text{e}^-$  occurs at 0 V vs.  $\text{Li}/\text{Li}^+$  under standard temperature and pressure conditions [86]. Therefore, the free energy of  $\text{Li}^+ + \text{e}^-$  is defined as  $-eU$  relative to the Li crystal, where  $U$  is the electrode potential relative to  $\text{Li}/\text{Li}^+$ . This method is analogous to the computational hydrogen electrode model proposed by Nørskov et al. [87]. By determining  $\Delta G$  for the electrochemical reactions, we can calculate the equilibrium reaction voltage  $E$  using the equation  $\Delta G = -nFE$ , where  $n$  is the number of electrons involved in the reaction and  $F$  is the Faraday constant (96485 C/mol). The theoretical mass energy density ( $\varepsilon_m$ ) and specific capacity ( $C$ ) of an electrode material are essential for understanding its electrochemical performance. These quantities can be calculated using the following equations:

$$C = (n \times F) / 3.6m$$

$$\varepsilon_m = \Delta G / \sum M$$

where  $m$  is the mole mass of an electrode material,  $\sum M$  is the sum of mole masses of both anode and cathode materials.

Next, we aim to investigate the Li-S precipitation process on Li anodes using DFT and ab initio molecular dynamics (MD) simulations. Understanding this process is crucial for developing effective strategies to mitigate the undesired shuttle effects on battery performance. MD simulations will be carried out in the NVT ensemble with fixed temperatures and volumes. The objectives of our simulations include: 1) elucidating the atomic-level interactions between various Li-S species and Li electrode surfaces; 2) revealing the mechanisms of  $\text{Li}_2\text{S}$  film formation on electrode surfaces; 3) examining the effects of Li-S precipitation on battery performance; and 4) investigating the diffusion and dissolution of Li-S species in the electrolyte.

To address these objectives, DFT calculations will be performed to investigate the energetics and electronic structures of various Li-S species interacting with Li metal surfaces. The influence of vdW forces on the adsorption process will be considered by incorporating the D3 corrections in the simulations. These calculations will provide insights into the nature of sulphur interacting with the anode surface, as well as the energetics of the adsorption process. Furthermore, the influence of anode surface structures on the adsorption of Li-S species will be also studied. The nudged elastic band (NEB) method will be employed to calculate the minimum energy paths of  $\text{Li}_2\text{S}$  film formation on Li metal surfaces. [88] This method will enable the identification of the most energetically favorable reaction pathways and the associated transition states. By mapping out the energy landscape of the  $\text{Li}_2\text{S}$  film formation process, we

can gain a deeper understanding of the driving forces and barriers involved in this phenomenon.

Furthermore, the diffusion and dissolution of Li-S species in the electrolyte will also be investigated, which is essential for understanding the transport properties of these species and their impact on battery performance. Our simulations will employ an amorphous model of the electrolyte solution, considering the common solvent such as 1,3-dioxolane (DOL), mixed with ethylene carbonate (EC), and lithium salt bis(trifluoromethane)-sulfonimide (LiTFSI).

In addition to atomistic simulations using classical computers, we will also explore quantum computer simulations of small molecules relevant to battery applications. Utilizing the unitary coupled cluster with double excitations algorithm, our initial focus will be on simulating H<sub>2</sub>O and LiH molecules, which require up to 20 qubits within the current quantum computing resources. Moreover, we will benchmark the results obtained from quantum computer simulations against classical computer calculations using the CCSD and DFT methods. As quantum computer hardware and algorithms progress, we plan to employ more qubits and simulate larger systems, such as the Li<sub>2</sub>S molecule. In parallel, under Task 1.3, we will develop variational algorithms for the condensed phase by introducing a plane-wave ansatz. This approach will enable quantum computers to model the electrode and electrolyte materials, providing valuable insights into the design and optimization of battery technologies.

#### *Discovering novel materials for enhanced battery performance*

Through the above simulations, we expect to gain a deeper understanding of the Li<sub>2</sub>S precipitation process on Li metal anodes in Li-S batteries, paving the way for the development of novel binder or anchoring materials to mitigate the shuttling effect. With this objective, our primary focus will be on the potential of 2D materials, MXenes. These 2D materials exhibit unique properties and characteristics, including high surface area, excellent electrical conductivity, and abundant active sites, making them promising candidates as anchoring materials. To gain a comprehensive understanding of the interaction between Li-S species and 2D anchoring materials at an atomic level, we will employ DFT calculations and periodic models considering vdW interactions. There are several vdW functionals available, and it is crucial to accurately describe the vdW interactions for reliable results. We will benchmark the vdW functionals using DLPNO-CCSD(T) calculations and choose the best-performing functional for our simulations. Systematically investigating the adsorption of Li-S species on various 2D MXenes will follow.

There are numerous combinations of MXenes due to the diverse possibilities for the transition metals, carbon/nitrogen layers, and surface functional groups. This vast compositional space provides us opportunities to tailor the properties of MXenes for optimal performance in Li-S batteries. To evaluate the performance of different MXenes, we will apply DFT calculations to determine key properties, including adsorption energies, activation energies of decomposition, and electronic structures. Adsorption energies are associated to the strength of binding between the Li-S species and MXenes, while activation energies of decomposition will predict the feasibility of Li-S species decomposition on MXenes. Furthermore, analysing the electronic structures will help us understand the electronic conductivity and charge transfer that occurs during the interactions. By analysing interaction mechanisms between 2D anchoring materials and the Li-S species, we aim to suggest ideal anchoring materials that can further enhance Li-S battery performance.

### 6.1.3. Implications

Atomistic models for battery materials have significant implications for improving the understanding of the behaviour and performance of Li-S batteries. Valuable insights into the understanding of binding strength, configuration distortion, charge transfer at an atomistic level, revealing the mechanism behind the anchoring effect, identifying ideal anchoring materials, and improving Li-S battery performance can be obtained through suggested methods and simulations modelling the dissolution of intermediate lithium polysulfide into the electrolyte.

Density Functional Theory (DFT) is widely used in battery modelling due to its scalability and relatively low computational cost. However, DFT has limitations in describing charge transfer states and capturing strong electron correlation effects. To overcome these limitations, higher-level *ab initio* methods such as CC or MRCI are required. These methods can provide more accurate descriptions of processes occurring on electrodes, but their computational complexity grows exponentially when more electrons are included, making them computationally expensive.

The development of quantum computing offers the potential to solve these problems by enabling the use of multi-reference methods and high-level *ab initio* methods at a faster rate. The implication of developing algorithms to simulate battery materials on an atomistic level using quantum computers includes a significant speed-up of calculation, higher accuracy due to more precise methods, and more accurate descriptions of processes between species. This can lead to a deeper understanding of electrochemistry at the interface between cathode and electrolyte and anode and electrolyte.

However, in the near term, the performance of quantum hardware is limited, and therefore only small or toy systems like LiH or LiH<sub>2</sub> can be simulated on quantum computers. The more distant goal and implication is when sufficient quantum hardware is available to simulate larger molecules e.g., stepwise decomposition of Li<sub>2</sub>S<sub>8</sub> and more complex systems like the influence of vdW forces on the adsorption process on Li metals, allowing a more detailed and accurate understanding of the chemistry and electrochemistry involved in battery materials.

In conclusion, the implication of developing atomistic models of battery materials using quantum computing is significant. The speed-up of calculation and higher accuracy due to more precise methods will allow for a more accurate description of the behaviour and performance of Li-S batteries. The deeper understanding of electrochemistry at the interface between cathode and electrolyte as well as anode and electrolyte will allow the identification of new materials and technologies that can improve the performance of Li-S batteries. It can help researchers in the field of battery technology make new discoveries and advance the field. By simulating different materials and their properties, researchers can develop new theories and hypotheses that can lead to new breakthroughs in the field. Overall, the development of atomistic models using quantum computing will play a crucial role in advancing the field of energy storage and improving the sustainability of our society

### 6.1.4. Impact on stakeholders

The impact of stakeholders on the development of atomistic models of battery materials on quantum computers is significant, particularly for institutions such as DLR and Fraunhofer. While it is not expected that quantum computers will replace current simulation methods like DFT in the near term, they offer a promising starting point for future development of battery material simulations on quantum computers.

One potential benefit of using quantum computers for atomistic modelling of battery materials is the ability to describe more accurate energy barriers, which can help researchers understand the driving forces for electrochemical processes. This can provide a deeper understanding of the electrochemistry at the interface between cathode, electrolyte and anode.

Additional direct stakeholders like PASQAL are working to develop real-world applications and proof of algorithms for quantum chemistry. An important consideration for these stakeholders is whether the algorithms used for quantum chemistry are as good as or better than classical algorithms. The potential for improvement of algorithms based on the calculation of more complex systems, including subject matter expert knowledge, is another important consideration for stakeholders in the development of atomistic models of battery materials on quantum computers.

In addition to the direct stakeholders from the Equality consortium, there are also indirect stakeholders, for whom the development of new battery materials using quantum chemical methods like DFT or CCSD(T) can have a significant impact on a wide range of stakeholders. Battery manufacturers, battery material suppliers, research institutions, end-users, automotive and aerospace industries, and government agencies all have a stake in the development of new battery materials that are more efficient, durable, and environmentally friendly. By using quantum chemical methods to design and evaluate new materials, researchers can identify materials that are suitable for use in batteries with greater precision and accuracy. Examples are the investigation of the shuttling effect in Li-S batteries or the diffusion and dissolution of Li-S species in the electrolyte. Understanding these processes can lead to the development of batteries that are more efficient, longer lasting, and more affordable, which can benefit end-users and battery manufacturers alike. Additionally, the use of simulation tools can help battery material suppliers identify new materials and improve their production processes. Finally, investors can benefit from the results of this research by making informed investments in companies that develop and produce these new battery materials.

Battery manufacturers are one of the primary stakeholders for material discovery simulation for battery materials. They can use the quantum chemical methods to develop new and better battery materials that can improve the performance, efficiency, and durability of their products. With atomistic simulation tools battery manufacturers can streamline their research and development processes, allowing them to bring new and improved batteries to market faster. This can give them a competitive advantage over other manufacturers and improve their bottom line. Simulation tools can also help them reduce costs by identifying materials that are more efficient and less expensive to produce. They may also benefit from the increased demand for Li-S batteries as they become more widely adopted in various applications, such as electric vehicles and stationary energy storage systems.

Researchers in the field of battery technology can also benefit from the development of fast quantum chemical calculations. Consequently, research institutions can leverage atomistic simulations to push the boundaries of battery technology, by identifying novel materials and properties, testing different hypotheses, and making more precise predictions about the behaviour of battery materials. As a result, this technology has the potential to drive ground-breaking discoveries and advancements in the field of battery technology.

In addition to the stakeholders, government agencies that provide funding for battery technology research can also benefit from atomistic calculations. By utilizing the results of such simulations, they can assess the viability of various research proposals and make well-informed decisions about which projects to fund. Moreover, they can leverage the quantum chemical simulation tools to evaluate the environmental and societal impact of different battery

technologies and make informed decisions about which technologies to support. In conclusion, the utilization of such methods can foster the development of more sustainable and efficient battery technologies, which can have a positive impact on society at large.

Battery Material Suppliers can use quantum chemical calculations to identify novel and improved materials that they can supply to battery manufacturers, ultimately resulting in more efficient and cost-effective batteries.

Moreover, the automotive industry, a major user of batteries, can develop better and more efficient batteries for their vehicles by using the results of quantum simulations. This is particularly important for electric vehicles, as improved batteries can lead to better performance and longer range, making them more competitive with traditional combustion engines. Furthermore, simulations can aid in the identification of materials that are more affordable and readily available, thus reducing production costs.

Similarly, the aerospace industry can benefit from these tools by developing more durable and efficient batteries that can withstand extreme environments, making them suitable for use in satellites and other space applications. The software can also help reduce the weight of batteries, which is critical for space applications where every gram counts.

End-users of battery-powered products, such as electric cars, mobile phones, and laptops, can benefit from quantum simulations by having access to better and more efficient batteries. Manufacturers can develop batteries with higher energy density and longer lifetimes, leading to longer battery life and reduced energy consumption, which is particularly important as concerns for environmental sustainability continue to grow.

## 6.2. Atomistic models for fuel cell simulation

### 6.2.1. Problem scenario description

To mitigate CO<sub>2</sub> emissions in civil aviation, hydrogen is considered a highly promising alternative fuel for powering aircraft. This is due to its potential for low CO<sub>2</sub> generation when produced from renewable energy sources and its primary by-product being water. The electrochemical oxidation within a SOFC is generally a conversion with maximum preservation of potential technical work. SOFCs promise significant reductions in the fuel consumption, noise and emissions.

Current state-of-the-art SOFCs are based on the anode and electrolyte supported cells. For lightweight applications, the anode supported tubular SOFC design is adopted with a thin anode support. This approach enables the manufacture of a thin electrolyte layer (8 mol% YSZ), which results in a low ionic resistance for the oxide transport and leads to high cell performance. Ni-YSZ is an exceptional anode material for SOFCs, as it exhibits extraordinary catalytic activity towards the hydrogen oxidation reaction. The electrochemical reaction occurring at the TPB of the anode can be expressed as follows:  $\text{H}_2 + \text{O}^{2-} \rightarrow \text{H}_2\text{O} + 2\text{e}^-$ . The cathode is a thin, porous layer on the electrolyte where oxygen reduction takes place. La<sub>0.6</sub>Sr<sub>0.4</sub>CoO<sub>3</sub> (LSC) serves as a mixed ionic and electronic conductive cathode material, providing the highest ionic and electronic conductivity among all SOFC cathode materials. A silver layer is coated as current collector layer (CCL) on top of the cathode to minimize electric in-plane conduction losses. The electrochemical reaction can be represented as follows:  $0.5\text{O}_2 + 2\text{e}^- \rightarrow \text{O}^{2-}$ .

In addition to the cells, the interconnectors are another main component of planar SOFC stacks. The metallic interconnector is used to electrically connect each cell of the stack to its neighbour cell and furthermore to separate the fuel from the air gas channel of two

neighbouring cells. The electrical current is hereby transferred in a perpendicular direction to the cell area. The interconnector can take up to 70% of the total weight of a planar stack. The SOFC is a high temperature fuel cell that operates at temperatures between 650 and 850°C. Unfortunately, such high operating temperatures lead to issues such as electrode sintering and costly interconnect materials, significantly hampering the commercial applications of SOFCs. As a result, the SOFC community has shifted its focus towards lowering the operating temperature to intermediate levels [89]. In practice, however, lowering the temperature will unavoidably lead to a significant performance loss, mainly due to the low reaction rate of the O<sub>2</sub> reduction at lower temperatures. Consequently, addressing these limitations remains a challenge for the SOFC community. To improve the performance of SOFCs, a deeper understanding of the fundamental electrochemical processes is essential. Atomistic simulations can provide valuable insights into the anode and cathode electrochemistry at the TPB, as well as the ionic transport in ceramic electrolytes. The primary goal is to increase the SOFC's power density by improving transport processes through operational measures and innovative material compositions. In this context, gaining a more fundamental understanding and optimization of the electrochemical processes is of particular interest, as will be demonstrated in the subsequent section.

### 6.2.2. Chosen methods

*Atomistic simulations of H<sub>2</sub> oxidation at the anode.*

The Ni-YSZ cermet is the most widely used material for SOFC anodes, as it possesses the essential qualities for an anode material, including good conductivity, catalytic activity, and stability. Our first research task will be the modelling of hydrogen oxidation at the TPB of a Ni cluster, YSZ, and a gas phase. We note that some simulation works have been done in this area [90,91]. These works will be used as a reference to evaluate the accuracy and reliability of our methods and models. Given that H<sub>2</sub> readily dissociates on the Ni surface, our primary focus will be on the water formation process, which proceeds through three possible pathways. These pathways for water formation at the TPB involve either the spill over of O or OH from YSZ to Ni or two consecutive spill overs of H atoms from Ni to YSZ. By using DFT and NEB methods, activation energy and reaction pathways will be computed. Subsequently, the rate-limiting step is identified, and our findings will be compared to existing literature results. The details of atomistic simulation using DFT methods have been described in 6.1.2.

*Atomistic simulations of O<sub>2</sub> reduction at the cathode.*

The performance of SOFCs is significantly affected by the electrochemical reaction rate of the ORR and the conductivity of cathode materials. Therefore, our focus will be on studying and understanding the cathode reaction in more detail. The possible reaction events during oxygen reduction processes can be divided into three categories [92]:

- (a) Surface reactions: i) Adsorption of O<sub>2</sub> molecules onto the LSC cathode surface. ii) Dissociation of O<sub>2</sub> molecules into O atoms. iii) Surface to bulk transport, where O atoms migrate from the surface into the bulk material. iv) Ionization, which involves the charge transfer of O atoms.
- (b) Transport mechanisms: i) Surface transport, where O atoms migrate along the cathode surface. ii) Bulk transport, where O atoms move through the bulk material. iii) Grain boundary transport, which involves the movement of O atoms along grain boundaries in the cathode material.
- (c) Electrolyte incorporation, where O atoms from the cathode material are incorporated into the YSZ electrolyte.



One technical challenge in modelling the ORR is that the GGA functional poorly describes the high-spin ground state of  $O_2$ . An empirical fitting method can be employed as a potential solution, where the ground state energy of  $O_2$  is obtained by  $E_{O_2} = E_{O_2(DFT)} + E_{O_2(corr)}$ . In this expression,  $E_{O_2(DFT)}$  represents the total energy of  $O_2$  computed by DFT, while  $E_{O_2(corr)}$  is an empirical correction term. This term can be determined by minimizing the error of formation enthalpy computed by DFT relative to experimental values for various metal oxides relevant to our study, such as perovskite.

To study the reaction events during oxygen reduction processes, we will construct a periodic slab model that represents the atomic structure of the cathode-electrolyte interface by placing LSC clusters on top of the YSZ support. This allows us to investigate the ORR occurring at the TPB. By performing a series of DFT calculations on this model, we can determine the energetics and kinetics of the various processes involved in the ORR, such as adsorption, dissociation, and transport.

Additionally, we will use the Bader method [93] to analyse charge transfer in ORR. This approach partitions the electron density of a system into atomic volumes using zero-flux surfaces, which are 2D surfaces where the charge density is a minimum perpendicular to the surface. In molecular systems, the charge density typically reaches a minimum between atoms, which serves as a natural place to separate atoms from each other. Since charge transfer is closely associated with the reaction events described earlier, employing the Bader method will enable us to better understand how charge is redistributed during processes like adsorption, dissociation, and ionization, and how this redistribution affects the efficiency of the ORR.

### 6.2.3. Implications

The implications of utilizing quantum computers for atomistic modelling of processes in solid oxide fuel cells (SOFCs) are noteworthy. The triplet state of the oxygen molecule in its ground state presents a challenge for conventional modelling methods. An open-shell method is required to accurately depict the energy of the  $O_2$  molecule and obtain precise reaction pathways. However, density functional theory (DFT) encounters difficulties in describing open-shell systems and necessitates correction terms to correctly describe the energies of oxygen reactions. Moreover, DFT cannot replicate the high-spin ground state of  $O_2$  and mandates an empirical correction term.

To obtain an accurate energy of  $O_2$  and the  $O_2$  reaction pathways, multiconfigurational methods such as MCSCF perform better. Nevertheless, these techniques are computationally expensive as the complexity grows exponentially when including more electrons.

Quantum computers possess the capability to solve multi-reference methods and high-level ab initio methods very swiftly. However, the current performance of quantum hardware is restricted, and as a result, only small or toy systems can be simulated on quantum computers.

The ultimate goal and implication of utilizing quantum computers for atomistic modelling of processes in SOFCs is when there is adequate quantum hardware available. At that point, it will be feasible to simulate more substantial and intricate systems with greater accuracy than what is presently achievable with classical computers. This will have a significant influence on the development of SOFCs and other areas of materials science research.

The development of algorithms to calculate ORR using quantum computers has significant implications. With the use of more precise methods on quantum computers, the accuracy of simulations can be improved, leading to a more accurate description of processes related to

oxygen reaction pathways. Moreover, utilizing quantum computers can enable a deeper understanding of electrochemistry at the interface between cathode and electrolyte and anode and electrolyte. This understanding can aid in the development of advanced materials for SOFC which are lighter and have a higher temperature stability.

#### 6.2.4. Impact on stakeholders

The modelling of atomistic processes in SOFCs, including processes like the ORR and cathode-electrolyte interface, has implications for stakeholders such as Airbus and Fraunhofer. Although it may not immediately replace current simulation methods like DFT, it can serve as a valuable starting point for investigation of multireference methods. By providing precise ground state energies of species within the ORR, quantum computers can help develop more accurate energy barriers and better understand the driving forces behind electrochemical processes within the fuel cell, potentially leading to alternative materials, which are lighter and more resilient for the application of SOFCs in airplanes.

Moreover, PASQAL, as a quantum computing company, can benefit from the real-world application and proof of algorithms for quantum chemistry. This can aid in determining the effectiveness of the algorithms in comparison to classical algorithms, and by continuously improving and stressing the algorithms with the calculation of more complex systems and subject matter expert knowledge, the quantum advantage can be demonstrated.

The simulation of challenging open-shell systems such as the oxygen molecule can be used to highlight this advantage, potentially leading to wider adoption of quantum computing in the field. The impact of this on indirect stakeholders such as the scientific community, other industries, and society is also noteworthy, as it can lead to a deeper understanding of fundamental chemical and physical processes, potentially leading to advancements in various fields.

## 7. Bibliography

- [1] A. Manthiram, Y. Fu, Y.-S. Su, *Accounts of chemical research* 46 (2013) 1125.
- [2] A.W. Harrow, A. Hassidim, S. Lloyd, *Physical review letters* 103 (2009) 150502.  
<<https://link.aps.org/doi/10.1103/PhysRevLett.103.150502>>.
- [3] F. Gaitan, *npj Quantum Information* 6 (2020) 61.
- [4] O. Kyriienko, A.E. Paine, V.E. Elfving, *Phys. Rev. A* 103 (2021) 52416.  
<<https://link.aps.org/doi/10.1103/PhysRevA.103.052416>>.
- [5] J. Sirignano, K. Spiliopoulos, *Journal of Computational Physics* 375 (2018) 1339.  
<<https://www.sciencedirect.com/science/article/pii/S0021999118305527>>.
- [6] K. Kubo, Y.O. Nakagawa, S. Endo, S. Nagayama, *Phys. Rev. A* 103 (2021) 52425.  
<<https://link.aps.org/doi/10.1103/PhysRevA.103.052425>>.
- [7] G. STEINBRECHER, W.T. SHAW, *Eur. J. Appl. Math.* 19 (2008) 87.
- [8] A.E. Paine, V.E. Elfving, O. Kyriienko, *Quantum Quantile Mechanics: Solving Stochastic Differential Equations for Generating Time-Series*, arXiv (2021).
- [9] F. G.S L. Brandão, R. Kueng, D. Stilck França, *Quantum* 6 (2022) 625.
- [10] Y. Cao, J. Romero, J.P. Olson, M. Degroote, P.D. Johnson, M. Kieferová, I.D. Kivlichan, T. Menke, B. Peropadre, N.P.D. Sawaya, S. Sim, L. Veis, A. Aspuru-Guzik, *Chemical Reviews* 119 (2019) 10856.
- [11] V.E. Elfving, M. Millaruelo, J.A. Gámez, C. Gogolin, *Phys. Rev. A* 103 (2021) 32605.  
<<https://link.aps.org/doi/10.1103/PhysRevA.103.032605>>.
- [12] V. Dunjko, Y. Ge, J.I. Cirac, *Physical review letters* 121 (2018) 250501.  
<<https://link.aps.org/doi/10.1103/PhysRevLett.121.250501>>.
- [13] Y. Ge, V. Dunjko, *Journal of Mathematical Physics* 61 (2020) 12201.
- [14] M. Rennela, S. Brand, A. Laarman, V. Dunjko, *Quantum* 7 (2023) 959.
- [15] D. Leichtle, L. Music, E. Kashefi, H. Ollivier, *PRX Quantum* 2 (2021) 40302.  
<<https://link.aps.org/doi/10.1103/PRXQuantum.2.040302>>.
- [16] B. Dunn, H. Kamath, J.-M. Tarascon, *Science (New York, N.Y.)* 334 (2011) 928.
- [17] M.M. Thackeray, C. Wolverton, E.D. Isaacs, *Energy Environ. Sci.* 5 (2012) 7854.
- [18] E.C. Evarts, *Nature* 526 (2015) S93-5.
- [19] J. Speirs, M. Contestabile, Y. Houari, R. Gross, *Renewable and Sustainable Energy Reviews* 35 (2014) 183.
- [20] H.-J. Peng, J.-Q. Huang, X.-B. Cheng, Q. Zhang, *Adv. Energy Mater.* 7 (2017) 1700260.
- [21] Z.W. Seh, Y. Sun, Q. Zhang, Y. Cui, *Chemical Society reviews* 45 (2016) 5605.
- [22] R. van Noorden, *Nature* 498 (2013) 416.
- [23] R. Fang, S. Zhao, Z. Sun, D.-W. Wang, H.-M. Cheng, F. Li, *Advanced materials (Deerfield Beach, Fla.)* 29 (2017).
- [24] M. Zhao, B.-Q. Li, X.-Q. Zhang, J.-Q. Huang, Q. Zhang, *ACS central science* 6 (2020) 1095.
- [25] T. Li, X. Bai, U. Gulzar, Y.-J. Bai, C. Capiglia, W. Deng, X. Zhou, Z. Liu, Z. Feng, R. Proietti Zaccaria, *Adv. Funct. Mater.* 29 (2019) 1901730.
- [26] M. Hagen, D. Hanselmann, K. Ahlbrecht, R. Maça, D. Gerber, J. Tübke, *Adv. Energy Mater.* 5 (2015) 1401986.
- [27] D.A. Boyd, *Angewandte Chemie (International ed. in English)* 55 (2016) 15486.
- [28] M.C. Williams, *Fuel Cells* 1 (2001) 87.
- [29] C.K. Dyer, *Journal of Power Sources* 106 (2002) 31.  
<<https://www.sciencedirect.com/science/article/pii/S0378775301010692>>.
- [30] Omar Z. Sharaf, Mehmet F. Orhan, *Renewable and Sustainable Energy Reviews* 32 (2014) 810. <<https://www.sciencedirect.com/science/article/pii/S1364032114000227>>.

- [31] A. Manthiram, S.-H. Chung, C. Zu, *Advanced materials* (Deerfield Beach, Fla.) 27 (2015) 1980.
- [32] Z. Wei Seh, W. Li, J.J. Cha, G. Zheng, Y. Yang, M.T. McDowell, P.-C. Hsu, Y. Cui, *Nature communications* 4 (2013) 1331.
- [33] M.A. Pope, I.A. Aksay, *Adv. Energy Mater.* 5 (2015) 1500124.
- [34] D.-W. Wang, Q. Zeng, G. Zhou, L. Yin, F. Li, H.-M. Cheng, I.R. Gentle, G.Q.M. Lu, *J. Mater. Chem. A* 1 (2013) 9382.
- [35] S. Kovetz, A. Kovetz, *Electromagnetic Theory*, Oxford University Press, 2000.
- [36] G. Lebon, D. Jou, J. Casas-Vázquez, *Understanding Non-equilibrium Thermodynamics*, Springer Berlin Heidelberg, Berlin, Heidelberg, 2008.
- [37] B.D. Coleman, W. Noll, *Rev. Mod. Phys.* 33 (1961) 239.  
<<https://link.aps.org/doi/10.1103/RevModPhys.33.239>>.
- [38] B.D. Coleman, W. Noll, *The Foundations of Mechanics and Thermodynamics: Selected Papers*. Springer Berlin Heidelberg, Berlin, Heidelberg, 1974, p. 145.
- [39] M. Schammer, V. Hoffmann, G. Pulletikurthi, T. Carstens, A. Lahiri, A. Borodin, B. Horstmann, A. Latz, F. Endres, *Phys. Chem. Chem. Phys.* 20 (2018) 4760.
- [40] M. Schammer, B. Horstmann, A. Latz, *J. Electrochem. Soc.* 168 (2021) 26511.
- [41] M. Schammer, A. Latz, B. Horstmann, *The journal of physical chemistry. B* 126 (2022) 2761.
- [42] M. Schammer, M. Lorenz, F. Kilchert, P. Nürnberg, A. Latz, B. Horstmann, M. Schönhoff, *The Journal of Physical Chemistry Letters* 13 (2022) 8761.
- [43] A. Latz, J. Zausch, *Electrochimica Acta* 110 (2013) 358.  
<<https://www.sciencedirect.com/science/article/pii/S0013468613011493>>.
- [44] R.B. Smith, M.Z. Bazant, *J. Electrochem. Soc.* 164 (2017) E3291-E3310.
- [45] T. Schmitt, A. Latz, B. Horstmann, *Electrochimica Acta* 333 (2020) 135491.  
<<https://www.sciencedirect.com/science/article/pii/S0013468619323631>>.
- [46] J. Newman, W. Tiedemann, *AIChE J.* 21 (1975) 25.
- [47] R. Hayes, N. Borisenko, M.K. Tam, P.C. Howlett, F. Endres, R. Atkin, *The Journal of Physical Chemistry C* 115 (2011) 6855.
- [48] W. Schmickler, *Journal of Solid State Electrochemistry* 24 (2020) 2175.
- [49] M.Z. Bazant, B.D. Storey, A.A. Kornyshev, *Physical review letters* 106 (2011) 46102.  
<<https://link.aps.org/doi/10.1103/PhysRevLett.106.046102>>.
- [50] J.P. Neidhardt, D.N. Fronczek, T. Jahnke, T. Danner, B. Horstmann, W.G. Bessler, *J. Electrochem. Soc.* 159 (2012) A1528-A1542.
- [51] B. Bauer, S. Bravyi, M. Motta, G. Kin-Lic Chan, *Chemical Reviews* 120 (2020) 12685.
- [52] H.-P. Cheng, E. Deumens, J.K. Freericks, C. Li, B.A. Sanders, *Frontiers in Chemistry* 8 (2020) 587143. <<https://www.frontiersin.org/articles/10.3389/fchem.2020.587143>>.
- [53] M.I. Dyakonov, *Future Trends in Microelectronics*. John Wiley & Sons, Ltd, 2013, p. 266.
- [54] B. Samaniego, E. Carla, L. O'Neill, M. Nestoridi, *E3S Web Conf.* 16 (2017) 8006.
- [55] S. Dörfler, S. Walus, J. Locke, A. Fotouhi, D.J. Auger, N. Shateri, T. Abendroth, P. Härtel, H. Althues, S. Kaskel, *Energy technology (Weinheim, Germany)* 9 (2021) 2000694.
- [56] R.V. Bugga, S.C. Jones, J.-P. Jones, J. Pasalic, F.C. Krause, L. Torres, *Meet. Abstr. MA2016-02* (2016) 693.
- [57] D. Eberle, B. Horstmann, *Electrochimica Acta* 137 (2014) 714.
- [58] L. Zhang, Z. Xia, *The Journal of Physical Chemistry C* 115 (2011) 11170.
- [59] L. Zhang, Z. Xia, *The Journal of Physical Chemistry C* 115 (2011) 11170.
- [60] M. Winter, R.J. Brodd, *Chemical Reviews* 104 (2004) 4245.
- [61] G. Che, B.B. Lakshmi, E.R. Fisher, C.R. Martin, *Nature* 393 (1998) 346.

- [62] R. Jinnouchi, K. Kodama, T. Hatanaka, Y. Morimoto, *Physical chemistry chemical physics* : PCCP 13 (2011) 21070.
- [63] A.E. Russell, *Faraday Discuss* 140 (2008) 9.
- [64] J.X. Wang, F.A. Uribe, T.E. Springer, J. Zhang, R.R. Adzic, *Faraday Discuss* 140 (2008) 347-62; discussion 417-37.
- [65] M.Z. Bazant, *Accounts of chemical research* 46 (2013) 1144.
- [66] W.G. Bessler, S. Gewies, M. Vogler, *Electrochimica Acta* 53 (2007) 1782.  
<<https://www.sciencedirect.com/science/article/pii/S0013468607010353>>.
- [67] J.A. Keith, T. Jacob, *Angewandte Chemie (International ed. in English)* 49 (2010) 9521.
- [68] K.-S. Chen, I. Balla, N.S. Luu, M.C. Hersam, *ACS Energy Lett.* 2 (2017) 2026.
- [69] W. Luo, L. Zhou, K. Fu, Z. Yang, J. Wan, M. Manno, Y. Yao, H. Zhu, B. Yang, L. Hu, *Nano Letters* 15 (2015) 6149.
- [70] J. Hassoun, F. Bonaccorso, M. Agostini, M. Angelucci, M.G. Betti, R. Cingolani, M. Gemmi, C. Mariani, S. Panero, V. Pellegrini, B. Scrosati, *Nano Letters* 14 (2014) 4901.
- [71] M. Naguib, J. Come, B. Dyatkin, V. Presser, P.-L. Taberna, P. Simon, M.W. Barsoum, Y. Gogotsi, *Electrochemistry Communications* 16 (2012) 61.  
<<https://www.sciencedirect.com/science/article/pii/S1388248112000070>>.
- [72] Q. Tang, Z. Zhou, P. Shen, *Journal of the American Chemical Society* 134 (2012) 16909.
- [73] M. Naguib, M.W. Barsoum, Y. Gogotsi, *Advanced materials (Deerfield Beach, Fla.)* 33 (2021) e2103393.
- [74] D. Song, X. Chen, Z. Lin, Z. Tang, W. Ma, Q. Zhang, Y. Li, X. Zhang, *ACS Nano* 15 (2021) 16469.
- [75] W. Ren, W. Ma, S. Zhang, B. Tang, *Energy Storage Materials* 23 (2019) 707.  
<<https://www.sciencedirect.com/science/article/pii/S240582971930008X>>.
- [76] Y. Wang, X. Huang, S. Zhang, Y. Hou, *Small Methods* 2 (2018) 1700345.
- [77] D. Xiong, X. Li, Z. Bai, S. Lu, *Small* 14 (2018) e1703419.
- [78] Q. Zhang, Y. Wang, Z.W. Seh, Z. Fu, R. Zhang, Y. Cui, *Nano Letters* 15 (2015) 3780.
- [79] J.P. Perdew, K. Burke, M. Ernzerhof, *Physical review letters* 77 (1996) 3865.  
<<https://link.aps.org/doi/10.1103/PhysRevLett.77.3865>>.
- [80] S. Grimme, J. Antony, S. Ehrlich, H. Krieg, *The Journal of Chemical Physics* 132 (2010) 154104.
- [81] A.D. Becke, *The Journal of Chemical Physics* 98 (1993) 5648.
- [82] A.D. Becke, *Physical review. A, General physics* 38 (1988) 3098.  
<<https://link.aps.org/doi/10.1103/PhysRevA.38.3098>>.
- [83] C. Lee, W. Yang, R.G. Parr, *Physical review. B, Condensed matter* 37 (1988) 785.  
<<https://link.aps.org/doi/10.1103/PhysRevB.37.785>>.
- [84] Y. Guo, C. Riplinger, U. Becker, D.G. Liakos, Y. Minenkov, L. Cavallo, F. Neese, *The Journal of Chemical Physics* 148 (2018) 11101.
- [85] A. Altun, M. Saitow, F. Neese, G. Bistoni, *Journal of Chemical Theory and Computation* 15 (2019) 1616.
- [86] L. Peng, Z. Wei, C. Wan, J. Li, Z. Chen, D. Zhu, D. Baumann, H. Liu, C.S. Allen, X. Xu, A.I. Kirkland, I. Shakir, Z. Almutairi, S. Tolbert, B. Dunn, Y. Huang, P. Sautet, X. Duan, *Nature Catalysis* 3 (2020) 762.
- [87] J.K. Nørskov, J. Rossmeisl, A. Logadottir, L. Lindqvist, J.R. Kitchin, T. Bligaard, H. Jónsson, *The Journal of Physical Chemistry B* 108 (2004) 17886.
- [88] G. Henkelman, B.P. Uberuaga, H. Jónsson, *The Journal of Chemical Physics* 113 (2000) 9901.
- [89] Y. Zhang, R. Knibbe, J. Sunarso, Y. Zhong, W. Zhou, Z. Shao, Z. Zhu, *Adv. Mater.* 29 (2017) 1770345.

- [90] S.C. Ammal, A. Heyden, J. Phys. Chem. Lett. 3 (2012) 2767.
- [91] C.S. Cucinotta, M. Bernasconi, M. Parrinello, Physical review letters 107 (2011) 206103. <<https://link.aps.org/doi/10.1103/PhysRevLett.107.206103>>.
- [92] S.C. Singhal, K. Kendall, Design and Applications (2003) 197.
- [93] R.F. Bader, others, Clarendon: Oxford, UK (1990).